ELSEVIER

Contents lists available at ScienceDirect

Plant Stress

journal homepage: www.sciencedirect.com/journal/plant-stress





Potato cultivars use distinct mechanisms for salt stress acclimation

Michael Nicolas ^{a,b,*}, Jort Bouma ^a, Jan Henk Venema ^c, Hanneke van der Schoot ^d, Francel Verstappen ^a, Thijs de Zeeuw ^a, Sanne E. Langedijk ^{a,d}, Damian Boer ^a, Johan Bucher ^d, Marten Staal ^c, Ben Krom ^c, J. Theo M Elzenga ^c, Richard G.F. Visser ^d, Christa Testerink ^a, Rumyana Karlova ^{a,*}

- a Laboratory of Plant Physiology, Plant Sciences Group, Wageningen University & Research, 6708 PB, Wageningen, the Netherlands
- Laboratory of Plant Physiology, Centre for Ecological and Evolutionary Studies (CEES), University of Groningen, P.O. Box 11103, 9700 CC Groningen, the Netherlands
- ^d Plant Breeding, Wageningen University & Research, 6708 PB, 15, Wageningen, the Netherlands

ARTICLE INFO

Keywords:
Potato
Salt stress
Acclimation
Root
ABA
Suberin
Transcription factors

ABSTRACT

Soil salinity induces osmotic stress and ion toxicity in plants, detrimentally affecting their growth. Potato (Solanum tuberosum) suffers yield reductions under salt stress. To understand salt-stress resilience mechanisms in potatoes, we studied three cultivars with contrasting salt sensitivity: Innovator, Desirée, and Mozart. Innovator emerged as the most resilient under salt stress, displaying minimal reductions in growth and plant tolerance index with no tuber yield loss, despite notable water loss. Conversely, Desirée experienced a significant tuber yield reduction but maintained better water retention. Mozart showed a low plant tolerance index and high water loss. Interestingly, ions measurement across different tissues revealed that, unlike chloride, sodium does not accumulate in tubers under salt stress in these cultivars, suggesting existence of an active sodium exclusion mechanism. A whole root transcriptomic analysis of these cultivars revealed a conserved salt stress response between potato and Arabidopsis. This response includes activation of various abiotic stress pathways and involves sequential activation of various transcription factor families. Root analyses showed that Innovator has lower suberin and lignin deposition, along with stronger K⁺ leakage in control conditions, resulting in a higher early stress response and increased ABA accumulation shortly after salt stress induction. This could explain Innovator has a more divergent transcriptomic response to salt stress compared to Desirée and Mozart. Nevertheless, Innovator displayed high suberin and lignin levels and ceased K^+ leakage after salt stress, suggesting a high acclimation ability. Altogether, our results indicate that acclimation ability, rather than initial root protection against salt prevails in long-term salt-stress resilience of potato.

1. Introduction

Soil salinity is a worldwide problem that reduces crop biomass and yield, causing early senescence, and can lead to plant death (Ghosh et al., 2001; Jaarsma et al., 2013; Van Zelm et al., 2020). Factors contributing to salinisation include soil erosion, poor irrigation, drought, flooding and sea level rise. About 10% of arable soil and 25 to 30% of irrigated land are saline worldwide, and the situation is expected to worsen with climate change which threatens food security as the population grows (Dasgupta et al., 2009; Ivushkin et al., 2019; Shahid et al., 2018; Hassani et al., 2020; Nawaz et al., 2010; Dahal et al., 2019).

Salt impacts plant growth through osmotic and ion toxicity stresses.

Different phases can be distinguished from the early Na⁺ sensing to growth recovery. Early Na⁺ accumulation in root cells stimulates different short- and long-range Ca²⁺ waves, which, activate the SALT OVERLY SENSITIVE (SOS) pathway (Lamers et al., 2020). In this early response HKT1 channel is also activated to exclude Na⁺ from the cell when NHX ion transporters sequester it in the vacuole (Van Zelm et al., 2020). The remaining cytosolic Na⁺ physically competes with K⁺ but does not achieve its function, hence impacting intracellular K⁺ homeostasis. Plant cell regulates the Na⁺/K⁺ ratio according to the amount of Na⁺ to maintain cellular osmotic and turgor pressure (Zou et al., 2022; Duan et al., 2013). This early sensing phase is followed in the next few hours by a stop phase and a quiescent phase where auxin, ABA and

^{*} Corresponding authors.

 $[\]textit{E-mail addresses:} \ michael.nicolas@cnb.csic.es \ (M.\ Nicolas),\ rumyana.karlova@wur.nl \ (R.\ Karlova).$

^b Current address: Plant Molecular Genetics Department, Centro Nacional de Biotecnología-CSIC, Campus Universidad Autónoma de Madrid, Madrid, Spain

ethylene signalling play a major role, allowing cell transcriptional reprogramming for acclimation. This transcriptomic salt-stress response allows the initiation of the growth recovery phase where gibberellins, brassinosteroids, and jasmonic acid usually play a crucial role (Van Zelm et al., 2020). The salt-stress response also includes an increased regulation of apoplastic transport to the stele by a higher lignin deposition around endodermal cells, in the Casparian strip, involving several MYB transcription factors (Li et al., 2023; Calvo-Polanco et al., 2021). Likewise, a stronger suberin deposition in the cell wall decreases Na⁺ permeability (Barberon et al., 2016; Ranathunge and Schreiber, 2011). This new growth initiation requires photosynthetic carbon influx from the leaf, the source tissue (Ho, 1988; Sonnewald and Fernie, 2018). By reducing growth in sink organs, salt-stress decreases sugar unloading and hence sink strength which can lead to carbon starvation in case of severe salt stress (Smith and Stitt, 2007).

Potato (Solanum tuberosum) is the fourth major crop (FAO et al., 2017) and represents an important species for food security worldwide. Potato is a moderately salt-sensitive crop, exhibiting reduced tuber yield under saline conditions (Jaarsma and de Boer, 2018; Nawaz et al., 2010). Previous research identified cv. Innovator as a more tolerant cultivar in an in vitro assay, showing a lower growth reduction of shoot, roots and tubers at different salt concentrations (Ahmed et al., 2020), while Desirée was found to be more tolerant than cv. Mozart, displaying a higher vegetative growth and accumulating more proline and less H₂O₂ in hydroponics (Jaarsma et al., 2013). In addition to the traditional development of shoots, branches, and leaves, potato plants develop different peculiar belowground organs, namely stolons, tubers and adventitious roots. Stolons are underground branches from which the tubers emerge. Tuber formation occurs in the meristematic regions where sucrose is converted into glucose 6-phosphate, which is subsequently transported into the amyloplasts to be transformed into starch (Ewing and Struik, 1992). Potato plants usually develop from tubers, not seeds, and only produce adventitious roots. Three different kinds of adventitious roots can be distinguished (Kratzke and Palta, 1985); the basal roots, emerging from the base of the shoot underground; the stolon roots, which grow from the belowground shoot node along with the stolon; and the stolon-node roots, developing from the stolon nodes. Very little is known about how salt stress affects the belowground organs of potato, particularly their adventitious roots.

Here, based on the literature, we selected Innovator, Desirée, and Mozart as contrasting cultivars to further investigate their mechanisms of salt-stress tolerance. Our data showed that Innovator has a lower yield reduction in salt-stress conditions, which however, is linked with a higher water loss compared to Desirée. Interestingly, we found that tubers actively exclude Na⁺ ions but do accumulate K⁺ and Cl⁻ ions. Innovator is initially less protected against salt stress by displaying the lowest suberin and lignin depositions prior salt stress. However, it shows the strongest acclimation potential by adequately accumulating suberin and lignin and by reducing K⁺ leakage in roots, after experiencing a significant stress associated with a massive ABA accumulation in the roots. This suggests that fast suberin deposition under salt stress, rather than the initial amount, correlates with the degree of resilience of the cultivars. RNA-seq transcriptomic analysis showed that the dynamics of salt-stress response in roots are also different in Innovator. We identified several transcription factor families that temporally regulate the saltstress response in potato roots.

2. Materials and methods

2.1. Plant materials and growth conditions

 $S.\ tuberosum\ L.\ cvs.$ Desirée, Innovator and Mozart were propagated in vitro from single-node stem cuttings on Murashige and Skoog medium including vitamins (Duchefa Biochemie BV, Haarlem, the Netherlands) containing 2% sucrose and 0.6% plant agar, 0.05% MES (Duchefa Biochemie BV) in chambers at 24 °C in an LD photoperiod (16h light, 8h

dark). Plants were cut below the fifth node from the apex and placed in a new box for rooting over seven days before being transferred to the greenhouse (phenotyping and ions measurement experiments), Unifarm WUR conditions: 16h/8h light/dark with 21 °C/18 °C Day/night temperature and 60% humidity. For the hydroponic experiment, plants were rooted for 3 days before transfer to the hydroponic tank.

2.2. Plant phenotyping

Plants were transferred in 2l pot containing vermiculite (Agravermiculite no.3, Helza-Hobbyzaden). Growing conditions were 16h/8h light/dark with 21 °C/18 °C Day/night temperature and 60% humidity. Plants were watered with Hoagland solution (11 mM NO3, 1 mM NH4) with a dripping system (1 min every 12h for the first three weeks when plants were 7-8 nodes long and 2 min every 8h afterwards). Salt stress was induced three weeks after planting by adding salt to the Hoagland solution. NaCl concentration was increased every 2 days (50 mM, 75 mM, 100 mM, 125 mM, 150 mM, 175 mM, 200 mM in the Hoagland solution). Salt concentration of 200 mM was maintained until harvesting. Phenotype was monitored after 8 weeks after planting. Traits measured are: shoot length, shoot node number, shoot-leaves fresh and dry weight (FW, DW), aerial branches number, leaves Normalized Difference Vegetative Index (NDVI), primary stolon number, total number of stolon branches (secondary stolons), total stolon FW/DW, basal root FW/DW, tubers number and FW/DW, stolon node roots FW/DW. 12 plants per cultivar per treatment were used. A two-way ANOVA, including an evaluation of the significance of the interaction term (genotype:treatment), was performed using the R environment (packages: car, emmeans, DHARMa, and multcomp; Lenth, 2017; Hartig, 2024; Hothorn et al., 2025). The results of the two-way ANOVA are shown in Supplementary Table 1. When the p-value for the genotype:treatment (control vs. salt) interaction was significant, a Tukey's HSD test was conducted to identify groups with significant differences, and the adjusted p-values for pairwise comparisons are shown in Supplementary Table 1. If the genotype:treatment interaction was not significant but the main effects of genotype and/or treatment were significant, comparisons were made based on these main effects. Violin plots were generated using ggplot2 (Wickham et al., 2024).

2.3. Ion measurement

After phenotyping, roots were rinsed in distilled water to eliminate peripheral ions originating from the vermiculite. Leaves from the fourth and fifth nodes from the apex were selected for ion measurements. Following desiccation, dry tissues were finely ground using a hammer mill with a 1 mm sieve, as described in (Nguyen et al., 2013).

In order to have enough dry materials for the measurement (especially the stolons and stolon node roots) the twelve biological replicates obtained from phenotyping were combined in pairs, resulting in 6 final replicates per cultivar and condition. 40 \pm 3 mg of tissue powder was used except for stolon node roots of which 15 mg was used. Powders were ashed at 575 °C for 5 h. Ashed samples were dissolved by shaking for 30 min in 1 ml 3 M formic acid at 99 $^{\circ}\text{C}$ and then diluted with 9 ml Milli-Q water. The samples were shaken again at 80 °C for another 30 min. A final 500x dilution was subsequently prepared by mixing 0.3 ml sample solution (0.2 ml for the leaves) with 9.8 ml MiliQ to assess the Na⁺, K⁺, Cl⁻, and Ca2⁺ content of each root and leaf sample using Ion Chromatography (IC) system 850 Professional, Metrohm (Switzerland). Statistical analyses (two-way ANOVA) were conducted as described above (Section 2.2). Results of the ANOVA and adj. p-values of the pairwise comparisons are shown in Supplementary Table 1. Violin plots were generated using ggplot2 (Wickham et al., 2024).

2.4. Hydroponic experiment and sampling

We used a half-concentrated Murashige and Skoog including

vitamins and 0.05 mM MES (pH=5.8) as a nutrient solution which was refreshed every two days. The plants were grown in black hydroponic containers within a growth chamber under 16h/8 h light/dark light cycle at 21 °C, allowing roots to grow in the dark. In the combined RNA-seq andABA quantification experiment, salt stress (125 mM) was induced after 2 weeks at ZT4 (Zeitgeber time, 4 hours in light). Roots and leaves were collected at ZT10 (time point 6h) and the following day at ZT4 (time point 24h). Three biological replicates were used. In order to reduce biological variability and increase their homogeneity, each root or leaves biological replicate is composed of materials from three plants. Tissues were flash-frozen in liquid nitrogen and subsequently ground with a mortar. For the suberin quantification, salt stress (125 mM) was added to the media of two weeks old plants and roots were transferred to the fixation buffer after one week of salt stress.

2.5. RNA extraction and RNA-seq analysis

RNA was extracted with the FavorPrep Plant Total RNA Mini Kit (FAVORGEN). DNA was digested in the column with RNase-free DNase I (Roche). The samples were sent for sequencing at Novogene (Cambridge, UK). Quality of the RNAs were determined by Novogene by performing 1% Agarose gel electrophoresis Nanodrop, reading to check for RNA amount and purity, and Agilent 2100 bioanalyzer for RNA Integrating Number (RIN). All the samples had a RIN>4 with a flat baseline and were used for library production. Messenger RNAs were purified from total RNA using poly-T oligo-attached magnetic beads. After fragmentation, the first strand cDNA was synthesized using random hexamer primers followed by the second strand cDNA synthesis. The library was ready after end repair, A-tailing, adapter ligation, size selection, amplification, and purification. 150 bp paired-end sequencing (PE150 bp strategy, >20 million reads) was conducted using Illumina NovaSeq 6000 platform by Novogene (Cambridge, UK). Clean reads for subsequent analyses were obtained through raw data filtering, sequencing error rate check and GC content distribution check. Read quality was also assessed with FASTQC (Andrews, 2010) and MULTIQC packages (Ewels et al., 2016). Reads quality control results are available in Supplementary Table 4. Trimming of low-quality reads was processed with TRIM GALORE! (Krueger et al., 2023). Reads were mapped to the transcriptome of S. tuberosum v6.1 (Pham et al., 2020) using SALMON (Patro et al., 2017). Differential Expressed Genes were obtained from pairwise comparisons using the R package DESEQ2 (Love et al., 2014). Differentially expressed genes (DEGs) were selected with an adjusted p-value < 0.01. The potato orthologs of the Arabidopsis genes were found by performing a blastp analysis using the potato protein sequence (v6.1.working_models.pep.fa), available at the SpudDB webpage, (Pham et al., 2020) as query. We used a restrictive cut-off of E-value < E-05. The potato/Arabidopsis orthologs table is available as Supplementary Table 2, annotations are those of TAIR10. The Gene Set Enrichment Analysis (GSEA) test of overrepresentation was performed as described in (Nicolas et al., 2022; Subramanian et al., 2005). The different GSEA lists are available in the Supplementary Table 3 (Dinneny et al., 2008; Gifford et al., 2008; Iyer-Pascuzzi et al., 2011; Kinoshita et al., 2012; Lan et al., 2012; Li and Lan, 2015; Huang et al., 2017; Rymen et al., 2019; Leal et al., 2022; Brault et al., 2019; Nicolas et al., 2022; Lamers et al., 2023; Tarancón et al., 2017; Gonzali et al., 2006; Osuna et al., 2007; Baena-González et al., 2007; Sulpice et al., 2009). The Gene Ontology analysis was performed using the R package topGO (p-value<0.05; Alexa and Rahnenfuhrer, 2023). GO terms of each gene come from the Arabidopsis orthologs. The transcription factor list used for the transcription factor enrichment comes from the PlantTFDB v5.0 (Arabidopsis) and Supplementary Table 2 was used to identify the orthologs in potato. We performed a hypergeometric test to determine if the enrichment is statistically significant and selected with a p-value<0.05. Arabidopsis orthologs of the potato DEGs were determined using Supplementary Table 2. The RNA-seq data are available in the EMBL Biostudies database (accession number E-MTAB-14181). Table of the normalized count values is available as Supplementary Table 4.

2.6. ABA quantification

The whole root system was quickly sampled and flash-frozen in liquid nitrogen. Leaves from the fourth and fifth nodes from the apex were selected and flash-frozen. Five biological replicates were used to quantify ABA content in root and leaves. In order to reduce biological variability and increase their homogeneity, each replicate is a pool from three plants. Samples were ground in liquid nitrogen. About 17mg of root and 30mg of leaves were used for this quantification. ABA measurement was performed as described before Li et al. (2023). Ground samples were extracted with 1 ml of 10% methanol containing 100 nM stable isotope-labelled internal standards ([2H6]ABA). Abscisic acid was extracted and measured using a modified protocol (Floková et al., 2014) where a StrataX spe-column 30 mg/3 ml (Phenomenex) was used. Solvents were removed using a speed vacuum system (ThermoSavant). Liquid chromatography-tandem mass spectroscopy was used for the detection and quantification of ABA. Sample residues were dissolved in $100 \, \mu l$ acetonitrile /water (20:80 v/v) and filtered using a $0.2 \, \mu m$ nylon centrifuge spin filter (BGB Analytik). A Waters XevoTQS mass spectrometer equipped with an electrospray ionization source coupled to an Acquity UPLC system (Waters) was used to quantify hormones by comparing retention times and mass transitions with standards as previously described (Schiessl et al., 2019; Gühl et al., 2021). Chromatographic separations were performed using acetonitrile/water (+ 0.1 % formic acid) on a Acquity UPLC BEH C18 column (100 mm, 2.1 mm, 1.7 mm Waters) at 40 °C with a flowrate of 0.25 ml/min. The column was equilibrated for 30 minutes with the solvent (acetonitrile /water (20:80 v/v) + 0.1% formic acid). For analysis, 5 μ l of sample was injected, followed by an elution program in which the acetonitrile fraction linearly increased from 20% (v/v) to 70% (v/v) in 17 minutes. Between samples, the acetonitrile fraction was increased to 100% and maintained there for one minute to wash the column. Before injecting the next sample, the acetonitrile fraction was set to 20 % in one minute. A capillary voltage of 2.5 kV was used in combination with a source temperature of 150 °C and a dissolution temperature of 500 °C. A IntelliSmart MS Console (Waters) was used to optimize the cone voltage and multiple reaction monitoring was used for quantification (Schiessl et al., 2019). The IntelliSmart MS Console was used to set Parent-Daughter transitions. Peaks were analysed using Targetlynx software (Waters) and samples were normalized for the internal standard recovery and expressed relative to the sample fresh weight. A standard curve was used to convert peak area to pmol per mg of fresh weight. Violin plots were generated using ggplot2 (Wickham et al., 2024).

2.7. Suberin deposition quantification

Fixation, clearing and staining were done according to Ursache et al. (Ursache et al., 2018). 3 cm-long root tips were fixed in 4% PFA dissolved in phosphate buffer (PBS) for 1.5 hours in a vacuum. Roots were washed twice in PBS (10 min with gentle agitation). Afterwards roots were cleared in Clearsee (Kurihara et al., 2015) for four days in the dark. Auramine O staining was carried out by placing the root in ClearSee solution containing 0.5% Auramine O and 0.1% Calcofluor for 12 hours with gentle agitation. Nile Red staining was carried out by placing the root in ClearSee solution containing 0.05% Nile Red and 0.1% calcofluor. Acridine Orange staining was performed by incubating the root in $1~\mu M$ Acridine Orange solution for 12hours as described in (Li and Reeve, 2004). Roots were washed twice in ClearSee solution for 30 min. Fluorol Yellow 088 was performed by fixing the root in 20% methanol and 4% hydrochloric acid for 20 min in 60 $^{\circ}$ C. Roots were washed afterwards in 7% NaOH and 60% ethanol for 15 min at room temperature. Rehydration was done by successive EthOH baths of 5 min, decreasing from 40% EthOH to 20% EthOH and lastly 10% EthOH. Next, roots were stained in a 0.01% Yellow 88 (in methanol) and were shaken for 3 days at (350 rpm) in the dark. Roots received a counterstaining with a 0.05% Aniline Blue solution (0.5% in Milli-Q water), for about an hour and washed three times in Milli-Q water.

The samples were mounted on slides containing a drop of Clearsee solution. Subsequently, the slides were imaged with a Leica TCS SP5 HyD confocal microscope using a HC PL FLUOTAR 10x/0.30 DRY objective to examine areas 2 cm away from the root tip. The following settings were applied: XY=512 \times 512; 400 Hz; 1,00 AU pinhole and smart gain + smart offset: disabled. A HyD1 detector was being used on counting mode. For Calcofluor White imaging, an OPSL 405 laser (strength 2.0%) was used for the excitation, with a 418–458 nm detection range. Auramine O, Acridine Orange and Yellow088 signals were visualised with an OPSL 488 laser (strength 15%) and detected with a range band from 495–554 nm. The detection range for Nile red was set from 580–620nm.

At least 10 z-stacks images (10 focal plans) were captured for each image. Images of three different roots from each plant were taken. Image processing was performed using Fiji (Schindelin et al., 2012). Z-stack images were merged with the "sum slices" function. The root area was outlined and the mean intensity was measured. Background intensity outside the root region was also measured for quantification correction following the formula:

45 min to make them hydrophobic. K⁺-selective electrodes were backfilled with 200 mM KCl and front filled with potassium Ionophore I -Cocktail A (Sigma-Aldrich), then inserted in a holder filled with 200 mM KCl and calibrated with 0.25, 0.5 and 1,0 mM KCl. Only electrodes with a Nernst slope between -50 mV and -59 mV and a correlation coefficient of at least 0.999 were used. Prior to the measurements, the roots were mounted in a petri dish using bee wax and a piece of glass capillary and incubated for 1h in a bath solution containing 0.5 mM CaCl2 and 0.5 mM KCl. To determine the optimal distance from the root tip for measuring K+ fluxes, flux profiles along the distal 2 mm of the root of all three cultivars were taken with 250 µm increments from the root tip. K⁺ fluxes were measured for approximately 2 min at each position in a control bath solution without NaCl and after 1h of incubation in a 75 mM NaCl bath solution. The optimal distances for stable K⁺ flux analyses were established at 250, 500 and 500 µm from the root tip for Mozart, Desirée and Innovator, respectively, which are all located at the flanks of the net K⁺ efflux peak. At these distances, K⁺ fluxes from lateral roots of potato sprouts -both control and NaCl acclimated- were recorded in the bath solution without NaCl to record the baseline K⁺ flux values. After 5 min, 75 mM NaCl was added, and the NaCl-induced K⁺ flux was recorded for a subsequent 25 min. Five biological replicates per treatment and genotype were used. The data are presented as means, with error bars indicating standard deviations. To determine whether the pre-treatment

$$Intensity = \left\lceil (Area \times Mean) - \left((AreaBackground \times MeanBackground) \times \left(\frac{Area}{AreaBackground} \right) \right) \right\rceil \bigg/ Area = \left\lceil (Area \times Mean) - \left((AreaBackground \times MeanBackground) \times \left(\frac{Area}{AreaBackground} \right) \right\rceil \right] \bigg/ Area = \left\lceil (Area \times Mean) - \left((AreaBackground \times MeanBackground) \times \left(\frac{Area}{AreaBackground} \right) \right\rceil \right] \bigg/ Area = \left\lceil (AreaBackground \times MeanBackground) \times \left(\frac{Area}{AreaBackground} \right) \right\rceil \bigg/ Area = \left\lceil (AreaBackground \times MeanBackground) \times \left(\frac{Area}{AreaBackground} \right) \right\rceil \bigg/ Area = \left\lceil (AreaBackground \times MeanBackground) \times \left(\frac{Area}{AreaBackground} \right) \right\rceil \bigg/ Area = \left\lceil (AreaBackground \times MeanBackground) \times \left(\frac{Area}{AreaBackground} \right) \right\rceil \bigg/ Area = \left\lceil (AreaBackground \times MeanBackground) \times \left(\frac{Area}{AreaBackground} \right) \right\rceil \bigg/ Area = \left\lceil (AreaBackground \times MeanBackground) \times \left(\frac{Area}{AreaBackground} \right) \right\rceil \bigg/ Area = \left\lceil (AreaBackground \times MeanBackground) \times \left(\frac{Area}{AreaBackground} \right) \right\rceil \bigg/ Area = \left\lceil (AreaBackground \times MeanBackground) \times \left(\frac{Area}{AreaBackground} \right) \bigg/ Area = \left\lceil (AreaBackground) \times \left(\frac{Area}{AreaBackground} \right) \right\rceil \bigg/ Area = \left\lceil (AreaBackground) \times \left(\frac{Area}{AreaBackground} \right) \bigg/ Area = \left\lceil (AreaBackground) \times \left(\frac{Area}{AreaBackground} \right) \right\rceil \bigg/ Area = \left\lceil (AreaBackground) \times \left(\frac{Area}{AreaBackground} \right) \bigg/ Area = \left\lceil (AreaBackground) \times \left(\frac{Area}{AreaBackground} \right) \right\rceil \bigg/ Area = \left\lceil (AreaBackground) \times \left(\frac{Area}{AreaBackground} \right) \bigg/ Area = \left\lceil (AreaBackground) \times \left(\frac{Area}{AreaBackground} \right) \bigg/ Area = \left\lceil (AreaBackground) \times \left(\frac{Area}{AreaBackground} \right) \bigg/ Area = \left\lceil (AreaBackground) \times \left(\frac{Area}{AreaBackground} \right) \bigg/ Area = \left\lceil (AreaBackground) \times \left(\frac{Area}{AreaBackground} \right) \bigg/ Area = \left\lceil (AreaBackground) \times \left(\frac{Area}{AreaBackground} \right) \bigg/ Area = \left\lceil (AreaBackground) \times \left(\frac{Area}{AreaBackground} \right) \bigg/ Area = \left\lceil (AreaBackground) \times \left(\frac{Area}{AreaBackground} \right) \bigg/ Area = \left\lceil (AreaBackground) \times \left(\frac{Area}{AreaBackground} \right) \bigg/ Area = \left\lceil (AreaBackground) \times \left(\frac{Area}{AreaBackground} \right) \bigg/ Area = \left\lceil (AreaBackground) \times \left(\frac{Area}{AreaBackground} \right) \bigg/ Area = \left\lceil (AreaBackground) \times \left(\frac{Area}{AreaBackground} \right) \bigg/ Area = \left\lceil ($$

Signal intensity of five plants per cultivar and conditions were measured. Value of each biological replicate represents the mean value obtained from three roots. Five biological replicates were used for the Auramine 0 quantification and four for Yellow 088. Statistical analyses (two-way ANOVA) were conducted as described above in Section 2.2. Results of the ANOVA and adj. p-values of the pairwise comparisons are shown in Supplementary Table 1. Violin plots were generated using ggplot2 (Wickham et al., 2024).

2.8. NaCl-induced root K⁺ flux analysis using MIFE

Seed tubers of Desirée, Mozart and Innovator were sprouted in vermiculite in a greenhouse at 22 °C /18 °C Day/night set point temperatures, 40% relative humidity, a 14h/10h light/dark cycle at a minimum PPFD of 170 µmol/m²/s by adding a 50% Hoagland nutrient solution with a 1:1 NO3/NH4 ratio as N-source. At a stem size of about 10 cm, sprouts were carefully removed from the tuber and transferred to 30 L containers with an aerated 50% Hoagland nutrient solution. After 7 days of acclimation to the hydroponic culture, the NaCl concentration in half of the containers was gradually increased to 75 mM in three days, whereas sprouts in the other half of the containers were kept under control conditions without NaCl. Subsequently after 2 weeks, in which the nutrient solution was refreshed after the first week, primary laterals of the basal roots with a total length of 2–3 cm were collected for K⁺ flux analyses using the microelectrode ion flux estimation (MIFE) system (University of Tasmania, Hobart, Australia) as described by Staal et al. (2011). The microelectrodes were made by pulling borosilicate glass capillaries (0.86 mm internal diameter; Harvard Apparatus, Cambridge, UK) in a vertical pipette puller (L/M-3P-A, List Medical Electronics, Darmstadt, Germany) and transferred to a stove for 4h or overnight at 250 $^{\circ}$ C. They were salinized with 60 μL chlorotributylsilane 7 (Sigma-Aldrich Chemie GmbH, St. Louis, WA, USA) and kept in the stove for

has an effect on K⁺ flux, statistical analyses were conducted using GraphPad Prism 10 (Prism GraphPad Software, Boston, USA) and the "Confidence Intervals of Parameters" method (Motulsky and Brown, 2006). Two different approaches were used, the Extra sum-of-squares F test and the Akaike's criterion (AIC; Cavanaugh and Neath, 2019; Motulsky and Christopoulos, 2004). The Extra sum-of-squares is based on traditional statistical hypothesis testing and is used for least-squares regression. When p-value is small, the simpler model (the one with few parameters) is wrong and accept the more complicated model. AIC approach does not use a hypothesis testing and hence does no generate a p-value. This method expressed a probability that each model is correct.

For Desiree and Mozart, the null hypothesis - that the exponential decay curves fitted to fluxes after NaCl addition are identical for roots in control conditions or those pre-treated with salt - cannot be rejected. In contrast, for Innovator, the null hypothesis is rejected indicating significant differences between the curves of control and pre-treated roots. In the case of Innovator, both AIC (probability <0.1%, AICc =21.76) and the extra sum-of-squares F-test (p<0.0001, F(DFn=2, DFd=14) =28.15) indicate that the data are better represented by two separate curves.

3. Results

3.1. Innovator is the most resilient cultivar but displays significant waterloss in response to salt

Previous studies indicated Mozart as salt-sensitive while Desirée and Innovator were identified as more resilient cultivars (Jaarsma et al., 2013; Ahmed et al., 2020). To further investigate the mechanisms of salt-stress resilience in potato we studied the effect of a progressive salt-stress initiated three weeks after transfer to the greenhouse (75 mM to 200 mM, and then maintaining at 200 mM onward). After eight weeks, all cultivars showed reduced shoot length, node number in salt-stress condition but the shoot-branch number remained unchanged

M. Nicolas et al. Plant Stress 15 (2025) 100798

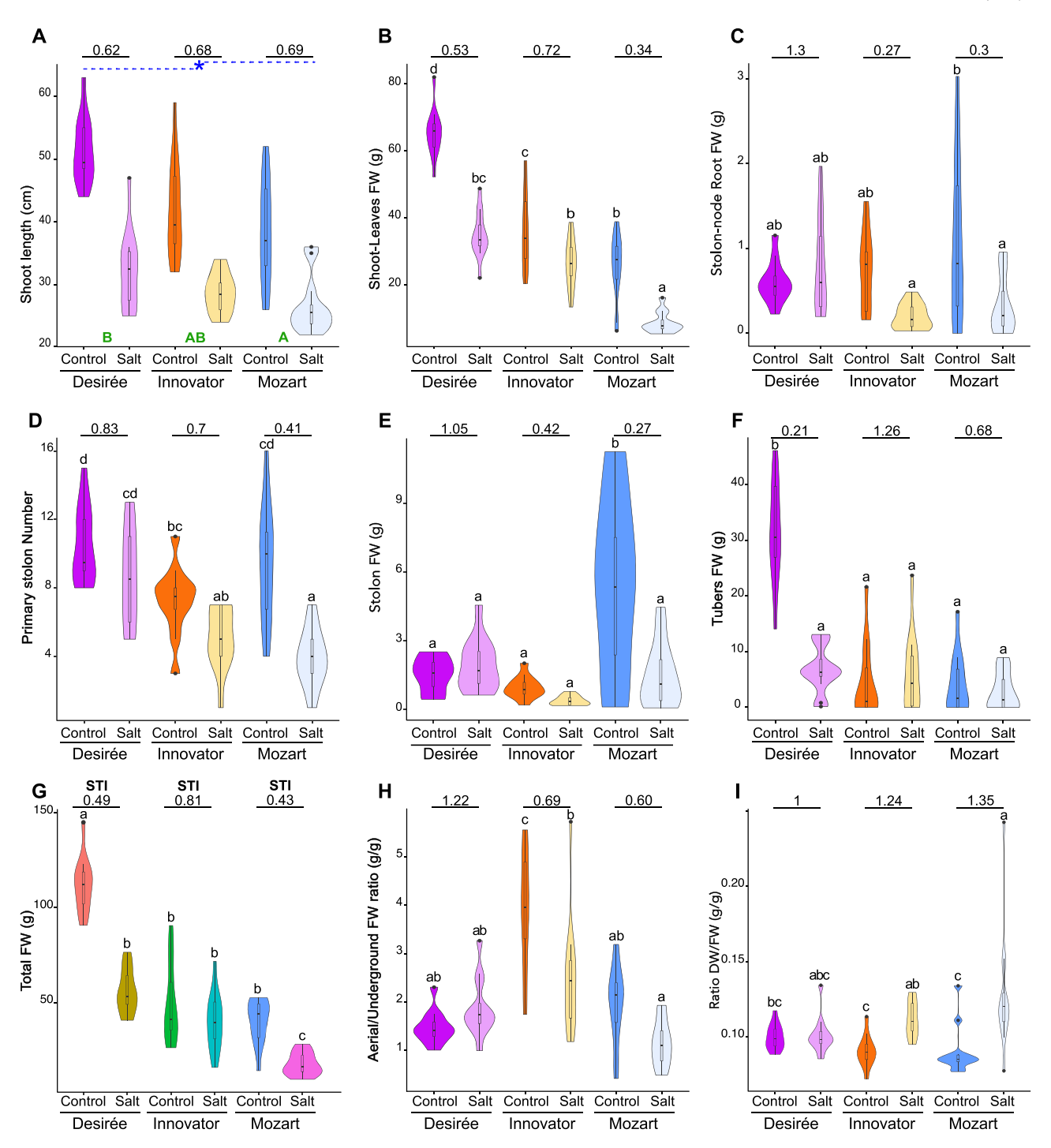


Fig. 1. Phenotype of Desirée, Innovator and Mozart potato plants in salt stress conditions. Plants were grown in the greenhouse and phenotype monitored after 8 weeks. Salt stress was induced three weeks after planting and NaCl concentration was increased every 2 days (50 mM, 75 mM, 100 mM, 125 mM, 150 mM, 175 mM, 200 mM). Thereafter, the salt treatment was maintained until the end of the experiment. (A-I) Violin plots representing diverse above and below ground phenotypes (n=12). A) length of the shoot. (B, C, E-G) Fresh weight (FW) of the shoot and leaves (B), stolon-node root (C), stolon (E), tubers (F) and total (salt-tolerance index, STI; G). (D) number of primary stolons emerging from the shoot below ground. (H) ratio of aerial part (shoot and leaves) FW to below ground FW (including basal and stolon-node roots, stolons and tubers). (I) ratio of dry weight (DW) to FW as indicator of the water retention. Value above each Control-Salt plot represents the ratio of salt to Control. Lowercase letters indicate differences significant differences among means (Tukey's HSD) when the interaction genotype:treatment was significant (P<0.05). When the interaction is not significant (P>0.05), green capital letters indicate differences between genotypes when significant (P<0.05), and a blue asterisk indicate differences between treatments (control/salt) when significant (P<0.05). Results of the statistical tests are shown in Supplementary Table 1.

(Fig. 1A; Supplementary Figs. 1A, 1B; Supplementary Table 1). Salt stress also reduced the leaf and main shoot fresh weight (FW) and the leaf Normalized Difference Vegetative Index (NDVI; Fig. 1B; Supplementary Fig. 1C; Supplementary Table 1). Among the three cultivars, Innovator was the least affected by the salt stress as illustrated by its

lower reduction of leaf FW (Fig. 1B; Supplementary Table 1). Below-ground, the basal roots' FW remained unaffected but stolon node roots' FW was significantly reduced in Mozart (Fig. 1C; Supplementary Fig. 1D; Supplementary Table 1). Number of primary stolons, emerging from the main shoot, and number of secondary stolons, emerging from the

primary stolons, decreased, resulting in a decreased stolon's FW which was significant for Mozart (Fig. 1D, E; Supplementary Fig. 1E; Supplementary Table 1). Finally, salt-stress induced an increased tuber number which was linked to a significant yield reduction in Desirée, suggesting that the plants intend to produce more tubers to compensate the decrease of tuber's starch accumulation (Supplementary Fig. 1F; Supplementary Table 1).

Next, we calculated the salt-tolerance index (STI), the ratio of total fresh weight between salt and control conditions in order to evaluate how salt globally affects the cultivars. The data showed that Innovator has the highest STI followed by Desirée suggesting they are more tolerant than Mozart (Fig. 1G). We also calculated the ratio of fresh weight between aerial and underground parts to assess the effect of salt stress to biomass partitioning responses. In control conditions, Innovator plants had the highest aerial/underground ratio (Fig. 1H; Supplementary Table 1), suggesting a greater allocation of energy aboveground in this cultivar compared to Desirée which had the lowest. In salt-treated plants, this ratio decreased in Innovator and Mozart plants, mostly as a consequence of their more conserved tuber yield in salt-stress conditions. Likewise, Innovator and Mozart showed an increased dry weight DW/FW ratio of the entire plant suggesting that they displayed a lower water retention under salt stress than Desirée (Fig. 1I; Supplementary Table 1)

Ultimately, we performed a correlation analysis between the different traits. Aside the expected positive correlation between shoot and leaves traits, results showed several positive correlations between the different stolon traits, especially in Innovator and Mozart (Supplementary Figs. 1G, 1I). In particular, stolon weight and stolon root weight were correlated which suggested their growth is highly linked. Interestingly, tuber traits were correlated with leaf weight in Desirée and Innovator, reaffirming the link between sugar production and tuber production. The association with any other underground part is however more complex.

In summary, this phenotypic analysis highlights the differential responses and plasticity of the three cultivars to salt stress. Desirée, despite having the second-highest STI, experienced significant reduction in leaf weight and tuber yield but maintained overall a good water content and a slightly higher tuber yield. Conversely, Innovator and Mozart, which initially have a carbon allocation turned towards the aerial part, exhibit similar yields under both control and salt-stress conditions, particularly Innovator. Mozart does not represent an interesting cultivar because of its low STI, lower tuber yield even in control conditions and its stronger water loss. On the other hand, Innovator emerges as an interesting resilient cultivar with the highest STI and an unchanged tuber yield in salt stress although this resilience is associated with a significant waterloss under salt stress. Combining Innovator's yield stability with Desirée's higher yield potential could provide significant benefits in agriculture.

3.2. Tubers do not accumulate sodium under salt stress

In addition to the traditional shoot, leaf and root tissues, potato plants develop different underground organs like stolons, stolon node roots and tubers all in contact with salt in the soil. To determine whether these organs differentially accumulate toxic ions under salt stress, we measured the ion contents of the different organs after the plant phenotyping (Fig. 1). As expected, sodium (Na⁺) and chloride (Cl⁻) contents were significantly increased in the two kinds of root as well as in the stolon of the three cultivars (Fig. 2A, 2B, 2C; Supplementary Table 1). Na⁺ concentration also rose in Mozart and Innovator aerial part but remained unchanged in Desirée (Fig. 2D; Supplementary Table 1). Surprisingly, Na⁺ content in tubers showed no significant difference between cultivars while Cl⁻ concentration was consistently higher, suggesting the exclusion of Na⁺ from tubers in salt conditions (Fig. 2E; Supplementary Table 1). Interestingly, potassium (K⁺) content also increased in tubers resulting in a mildly decreased Na⁺/K⁺ ratio

(Fig. 2E; Supplementary Table 1), while K^+ decreased in basal roots and in stolon node roots, leading to an increased Na^+/K^+ ratio (Fig. 2A, 2B; Supplementary Table 1). This ratio increased in Innovator and Mozart leaves, due to their higher Na^+ and lower K^+ content (Fig. 2D; Supplementary Table 1). Calcium (Ca2 $^+$) decreased in Innovator and Mozart leaves which could be related to the increase Na^+ in this tissue of these two cultivars. Phosphate (PO₄2') and sulphate (SO₄2') concentrations remained unchanged between control and salt treatments, suggesting that they do not play any role in long term salt-stress adaptation (Supplementary Figs. 2A, 2E; Supplementary Table 1). Conversely, magnesium content was significantly decreased in the aerial part (shoot and leaves) of Mozart plants (Supplementary Fig. 2D; Supplementary Table 1) while it increased in stolons suggesting that it might have a role in salt-stress adaptation in this cultivar.

These results indicate varied strategies for Na⁺ accumulation among cultivars. Aboveground, Na⁺ likely accumulates in the leaves/stems of Innovator and Mozart. Belowground, root types and stolons accumulated Na⁺ which is actively excluded from the tubers that hence do not represent an additional organ for Na⁺ sequestration.

3.3. transcriptomic response of innovator indicates a more divergent acclimation

To understand in more detail the molecular mechanisms of the salt-stress response in the adventitious roots of the three cultivars, we conducted an RNA-seq transcriptomic analysis. We compared the transcriptomes of the basal roots of the three cultivars grown in control or salt-stress conditions (125 mM), 6h and 24h after stress induction. Principal component analysis (PCA) of the transcriptome revealed that after 6h, PC1 separated control and treated roots of Mozart and Desirée but not Innovator which also showed fewer differentially expressed genes (DEGs; Fig. 3A, 3B; Supplementary Table 5). After 24h of stress, PC1 marked a clear salt-stress response in all three cultivars, with Innovator showing the highest DEG number (Fig. 3A, 3B; Supplementary Table 5). The results suggested a dynamic acclimation process to salt stress across the cultivars.

The comparison of the DEGs between the cultivars showed that after 6h, 327 upregulated genes were shared between the three cultivars, while only 152 downregulated genes were shared (Fig. 3C). In order to identify the genetic pathways involved in salt-stress responses we performed a Gene Ontology (GO) enrichment analysis and a Gene Set Enrichment Analysis (GSEA) which is a statistical approach allowing the identification of over-represented gene sets among the up- and downregulated DEG (Supplementary Table 3; Subramanian et al., 2005). The shared upregulated genes expectedly showed an enrichment for several stress-related terms including water deprivation, salt stress, cold, wounding and osmotic stresses as well as K+ homeostasis (Table 1 and Supplementary Table 6). Consistently, GSEA revealed that down- and upregulated gene sets previously associated with Na⁺ stress response in Arabidopsis were accordingly enriched in our datasets, emphasizing the conservation of salt-stress response in plants (Fig. 4A; Supplementary Fig. 3; Dinneny et al., 2008; Lamers et al., 2023). Likewise, sets of genes related to different stresses were also found enriched, underlying the existence of a core gene set common between the different abiotic stress (Fig. 4A; Supplementary Fig. 3); Dinneny et al., 2008; Iyer-Pascuzzi et al., 2011; Lan et al., 2012; Rymen et al., 2019). Interestingly, Innovator displayed a milder stress response after 6h suggesting a distinct mechanism.

Additionally, both GO and GSEA analyses highlighted the importance of ABA and jasmonic acid signalling in salt-stress response after 6h (Table 1; Supplementary Table 6; Fig. 4A). GSEA also indicated a homogenous activation of the Strigolactones (SL) signalling pathways (Fig. 4A). On the other hand, GO and GSEA gene sets related to cell division and growth processes were logically downregulated (Fig. 4A; Table 1 and Supplementary Table 6). Likewise, plasmodesmata and root hair development gene sets were inactivated (Brault et al., 2019; Huang

M. Nicolas et al. Plant Stress 15 (2025) 100798

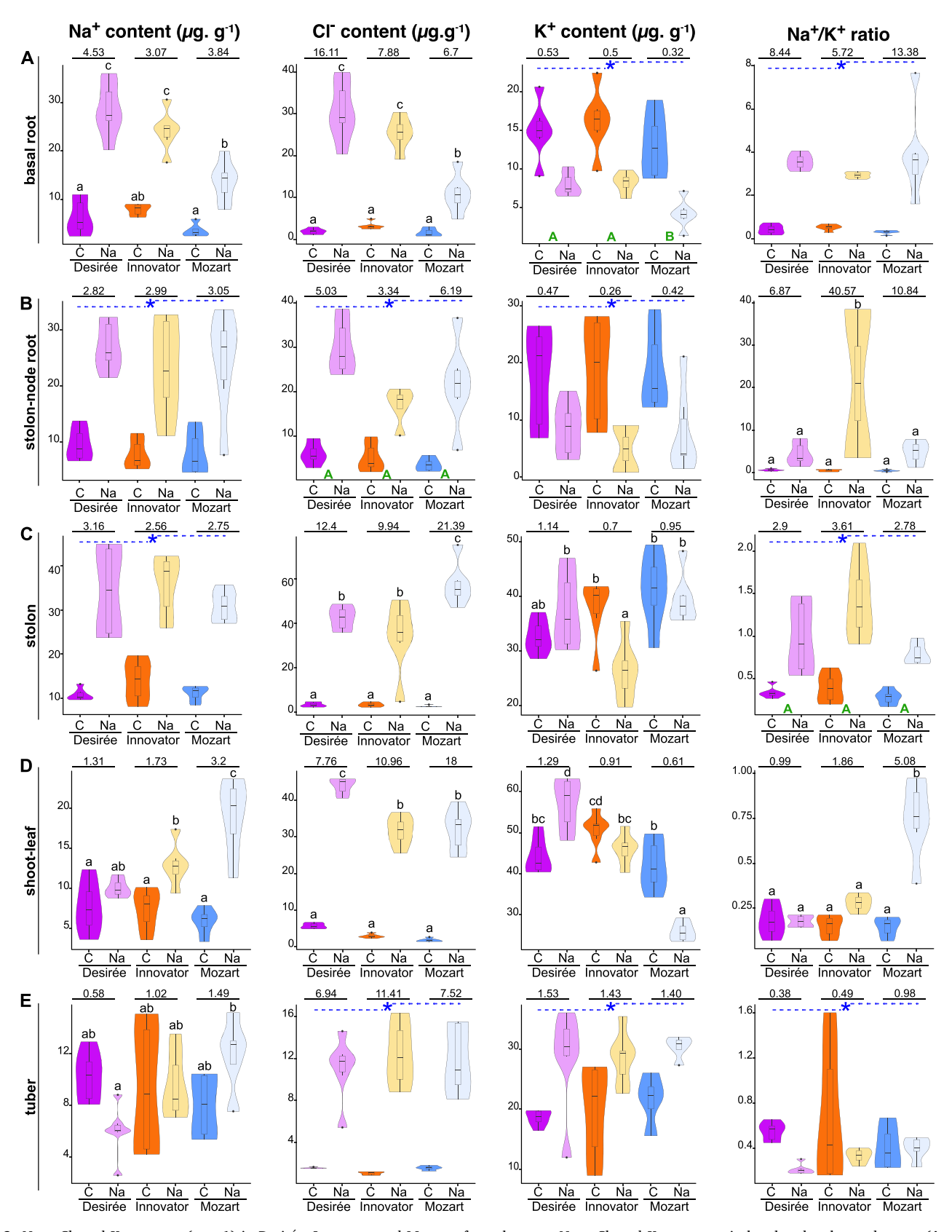


Fig. 2. Na+, Cl- and K+ content (μ g.g-1) in Desirée, Innovator and Mozart after salt stress. Na+, Cl- and K+ contents in basal and stolon-node roots (A and B respectively), stolon (C), shoot and leaves tissues (D) and tubers (E). Sample size is constituted by 6 replicates, each of them is a pool of two plants. Plants used are those of the phenotyping (Fig. 1) and grown in the greenhouse in control conditions (C) or with an increased NaCl stress (Na) up to 200 mM. Value above each Control-Salt plot represents the ratio of salt to Control ratio. Lowercase letters indicate differences significant differences among means (Tukey's HSD) when the interaction genotype:treatment was significant (P<0.05). When the interaction is not significant (P>0.05), green capital letters indicate differences between genotypes when significant (P<0.05), and a blue asterisk indicate differences between treatments (control/salt) when significant (P<0.05). Results of the statistical tests are shown in Supplementary Table 1.

M. Nicolas et al. Plant Stress 15 (2025) 100798

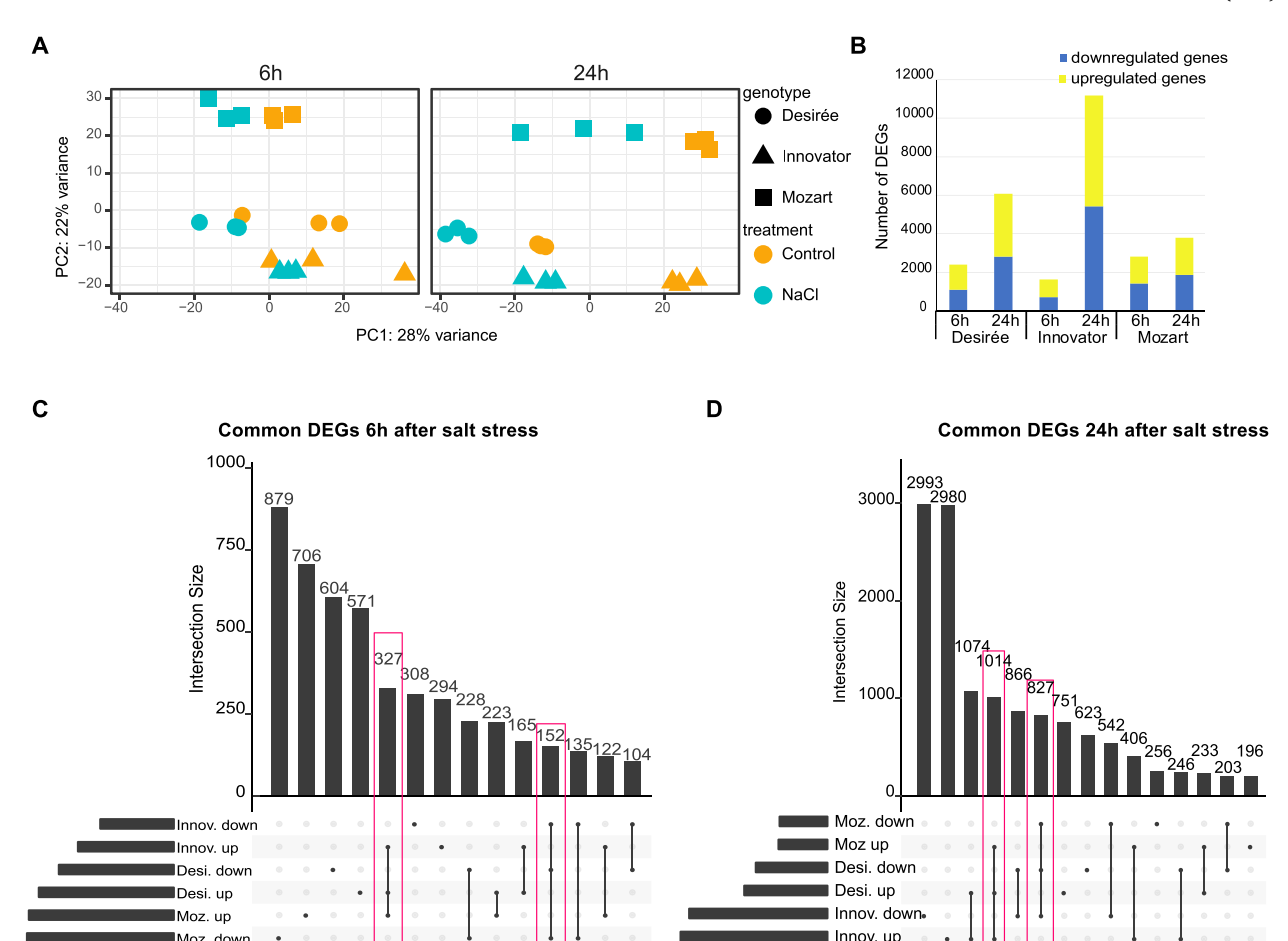


Fig. 3. Transcriptomic response in the roots of Desirée, Innovator and Mozart after salt stress (125 mM). A) Principal Component Analysis (PCA) of the salt stress response of the three cultivars (Desirée, Innovator, Mozart) at either 6h or 24h. B) Number of Differentially Expressed Genes (DEGs, adj-P<0.01) upregulated and downregulated at 6h and 24h after salt stress induction. (C-D) UpSet graph (Lex et al., 2014) showing common DEGs among the three cultivars, Desirée (Desi.), Innovator (Innov.) and Mozart (Moz.), and treatment at 6h (C) and 24h (D). The set size bars represent the total number of up- or downregulated DEGs in each cultivar at 6h or 24h. Dots below the barplots indicate the DEG sets that are included in the comparison. Values above the bars indicate the number of genes shared between the DEG sets. Red boxes highlight the shared DEGs up- and downregulated between the three cultivars at either 6h or 24h after salt stress induction.

6000

4000 2000

Set Size

et al., 2017) while suberin deposition genes (Leal et al., 2022) were activated indicating that the cellular acclimation aimed to limit Na⁺ absorption and diffusion in the roots (Fig. 4A). Interestingly, gene sets related to carbon starvation (Tarancón et al., 2017; Gonzali et al., 2006; Osuna et al., 2007; Baena-González et al., 2007; Sulpice et al., 2009) were found activated in Desirée and Mozart after 6h which is consistent with a lower sugar loading in the roots due to the growth arrest (Fig. 4A). Although cell proliferation gene sets are downregulated in Innovator, the carbon starvation gene sets are surprisingly also downregulated in this cultivar after 6h emphasizing the singular response dynamic of this cultivar.

Moz. down

1000 500

Set Size

After 24 hours exposure to salt stress, 1014 upregulated and 827 downregulated genes were found in common between the three cultivars (Fig. 3D). A continued activation of stress-related, suberin deposition and ABA signalling genes was consistently observed (Table 1; Supplementary Table 6 and Fig. 4A). Carbon starvation response was activated suggesting that it was previously delayed. GO terms analysis showed that lateral root growth, water and symplastic transport were downregulated which is consistent with the persistent inactivation of plasmodesmata and root hair growth genes sets observed (Table 1; Supplementary Table 6; Fig. 4A). Moreover, downregulation of ethylene and brassinosteroid (BR) signalling pathways was evident across cultivars (Fig. 4A), while cytokinin (CK), gibberellins (GA) and methyl jasmonate (MJ) were uniquely downregulated in Innovator which

further highlights its distinct response profile (Fig. 4A).

To identify which channel/transporter are involved in salt acclimation in potato roots, we investigated the expression pattern of the different channel/transporter genes identified. Results showed that SKOR/GORK K⁺⁻ efflux channel and AKT1 K⁺⁻ influx coding genes were upregulated during the stress response of the cultivars suggesting they play a role in the shared salt response (Supplementary Fig. 4). Interestingly, another SKOR/GORK gene (Soltu.DM.11G001630) was found more expressed in Innovator and down-regulated in salt-stress conditions. Moreover, several transporters from different classes like AKT1, HAK7, NHX5, NHX6 and KEA3 and KEA4 were specifically upregulated in Innovator after 24 hours indicating they may play an important role in the salt acclimation of this genotype.

Altogether, our transcriptomics data showed that the salt-stress response in potato exhibits a shared core mechanism with Arabidopsis and also has a part in common with other abiotic stresses. Innovator shows a unique temporal pattern coupled with a differential activation of stress-related pathways and channel /transporter genes which point to a distinct resilience strategy in this cultivar.

3.4. The different salt-stress response phases specifically involve different TF families

Because of their important roles in regulating gene networks, we

Table 1GO analysis of salt stress response. Gene Ontology (GO) analysis of salt stress response illustrating the ten most enriched biological process GO terms for DEG shared among three cultivars. The enriched GO terms for down-regulated and up-regulated genes are presented separately.

	common downregulated	p-value	common upregulated	<i>p</i> -value
6h	DNA replication initiation double-strand break repair via break- induced replication	6.10E- 11 2.60E- 06	response to water deprivation response to abscisic acid	1.40E- 13 2.70E- 11
	anatomical structure arrangement	6.20E- 06	response to salt stress	1.00E- 09
	nuclear DNA replication	7.70E- 06	positive regulation of syringal lignin biosynthetic process	1.30E- 08
	organic acid metabolic process	0.00018	response to oxidative stress	1.20E- 07
	plant organ morphogenesis	0.00083	defense response to fungus	7.60E- 07
	response to desiccation	0.00116	positive regulation of seed germination	2.10E- 06
	intracellular iron ion homeostasis	0.00135	response to wounding	2.60E- 06
	DNA unwinding involved in DNA replication	0.00152	JA and ethylene- dependent systemic resistance, ethylene mediated signaling pathway	7.00E- 06
	response to inorganic substance	0.00261	response to cold	1.30E- 05
24h	double-strand break repair via break- induced replication	1.20E- 07	response to water deprivation	6.10E- 15
	DNA replication initiation	1.40E- 07	response to abscisic acid	2.20E- 10
	macromolecule biosynthetic process	4.70E- 07	response to wounding	5.10E- 10
	cell wall biogenesis	5.90E- 07	cellular catabolic process	7.10E- 10
	plant-type cell wall biogenesis	1.70E- 05	organonitrogen compound catabolic process	1.30E- 09
	mitotic cell cycle process	4.70E- 05	cellular response to hypoxia	1.60E- 09
	unidimensional cell growth	6.30E- 05	response to oxidative stress	3.70E- 09
	microtubule cytoskeleton organization	9.00E- 05	response to salt stress	1.10E- 08
	plant-type cell wall organization or biogenesis	9.70E- 05	leaf senescence	1.20E- 07
	regulation of actin filament depolymerization	0.00013	defense response to bacterium	1.60E- 07

examined transcription factor (TF) family's enrichment in response to salt stress (Fig. 4B). We found distinct patterns emerging over time and across different cultivars. After 6h, the TALE (Three Amino acid Loop Extension), the MYB (MYeloBlastosis), and the HD-ZIP (Homeodomain-leucine Zipper) family were enriched in the shared upregulated genes suggesting a conserved early activation of these TFs in response to the stressor (Fig. 4B; Supplementary Table 7). In addition, the stress-related TF families WRKY, HSF (Trimerization of heat shock transcription factor) and ERF (Ethylene Responsive Factor) were enriched in Desirée suggesting an early activation of stress-adaptation pathways in this cultivar. After 24h, the TF landscape showed a more intricate picture. HD-ZIPs were subsequently downregulated indicating a specific role in the early stage of stress response (Fig. 4C; Supplementary Table 7). While TALE continued to be upregulated, additional stress-related TF families like HSF and WRKY were also enriched, along with GRAS and NAC

(NAM, ATAF1/2, and CUC2) which are usually involved in growth and development. This indicated a broader and more intensified transcriptomic response in roots, likely corresponding to the growth recovery phase. Interestingly, Innovator displayed unique TF enrichment patterns, confirming its major reprograming and recovery phase at this time point.

Altogether these results reveal a nuanced and cultivar-specific regulation of TFs within the first 24h of salt stress in the roots. The stress response first includes the recruitment of specific TF families like MYB and HD-ZIP at 6h of stress, followed by HSF, WRKY, NAC and GRAS at 24h, while TALE TF played a continuous role.

3.5. Innovator initially shows greater sensitivity to salt stress but adequately acclimates

Suberin and lignin can be deposited in the cell wall of specific root cells and acts as barriers preventing radial ion transport to the stele upon stresses (Barberon et al., 2016; Ranathunge and Schreiber, 2011; Doblas et al., 2017). In salt-stressed roots, Na+ content increased while K+ decreased, in particular in basal roots (Fig. 2A, 2B). GSEA showed that suberin gene set was activated in the three cultivars but that the intensity of the activation varies suggesting variation of suberin deposition (Fig. 4A). We therefore meant to confirm that suberin and lignin deposition occurs in salt-stressed potato roots. We stained Desirée basal roots with Nile Red and Yellow 88, specifically staining suberin; Auramine O that stains lignin, suberin and cutin; and Acridine orange which stains lignin, cutin, cellulose, DNA and the polyphenolic domain of suberin (Briggs and Morris, 2008; Kováčik et al., 2014; Houtman et al., 2016; Ursache et al., 2018). We could not detect any staining with Nile red (Supplementary Fig. 5A) while conversely, Yellow 88, Auramine O and acridine orange stained the differentiated zone of the root (Supplementary Fig. 5A). Orthogonal view of basal root stained with Auramine O indicated that the suberin and lignin deposition took place in the exodermis and in the Casparian strips (Supplementary Fig. 5B). We next quantified the suberin and lignin deposition of the roots of the three cultivars one week after salt-stress induction in vitro conditions using yellow 88 and Auramine O. In control conditions, both staining methods indicated that Mozart showed a higher suberin and lignin deposition compared to the other two cultivars suggesting that it may be more protected against salt absorption (Fig. 5A, 5B; Supplementary Table 1). However, after one week of salt treatment, these depositions were unchanged in Mozart's roots while Innovator roots adjusted their deposition levels under salt stress, eventually reaching levels comparable to those observed in Mozart suggesting that Innovator roots can adapt their suberin and lignin levels upon salt stress (Fig. 5A, 5B; Supplementary Table 1). This increased in Innovator's roots was in particular significant in the case of Yellow088 staining suggesting that suberin deposition is especially important for the root acclimation to salt stress in Innovator. Similarly, Desirée root acclimate to salt stress by increasing suberin and lignin deposition, nevertheless this accumulation did not reach the level of Mozart and Innovator under salt stress.

These results suggest that roots of Innovator and Desirée are conceivably less protected against sudden Na^+ stress than Mozart which hence could lead to a rapid Na^+ influx and osmotic stress. To explore whether this difference of suberin deposition can also influence the Nainduced K^+ efflux, we used a non-invasive microelectrode ion flux (MIFE) system to compare the K^+ efflux in response to NaCl addition (75 mM) in roots grown either in control or salt conditions. When roots are initially grown in control conditions, Innovator's roots showed a significant K^+ efflux after addition of salt which was not observed in Desirée or Mozart (Fig. 5C). However, after 14 days of salt-stress acclimation (75 mM), Innovator roots no longer exhibited this net K^+ efflux from root cells (flux curves of pre-treated roots significantly different from the control, p < 0.1%, with AICc method, p < 0.0001 with F-test, see methods 2.8 for more details), suggesting that Innovator can acclimate to NaCl by decreasing K^+ efflux under salt stress.

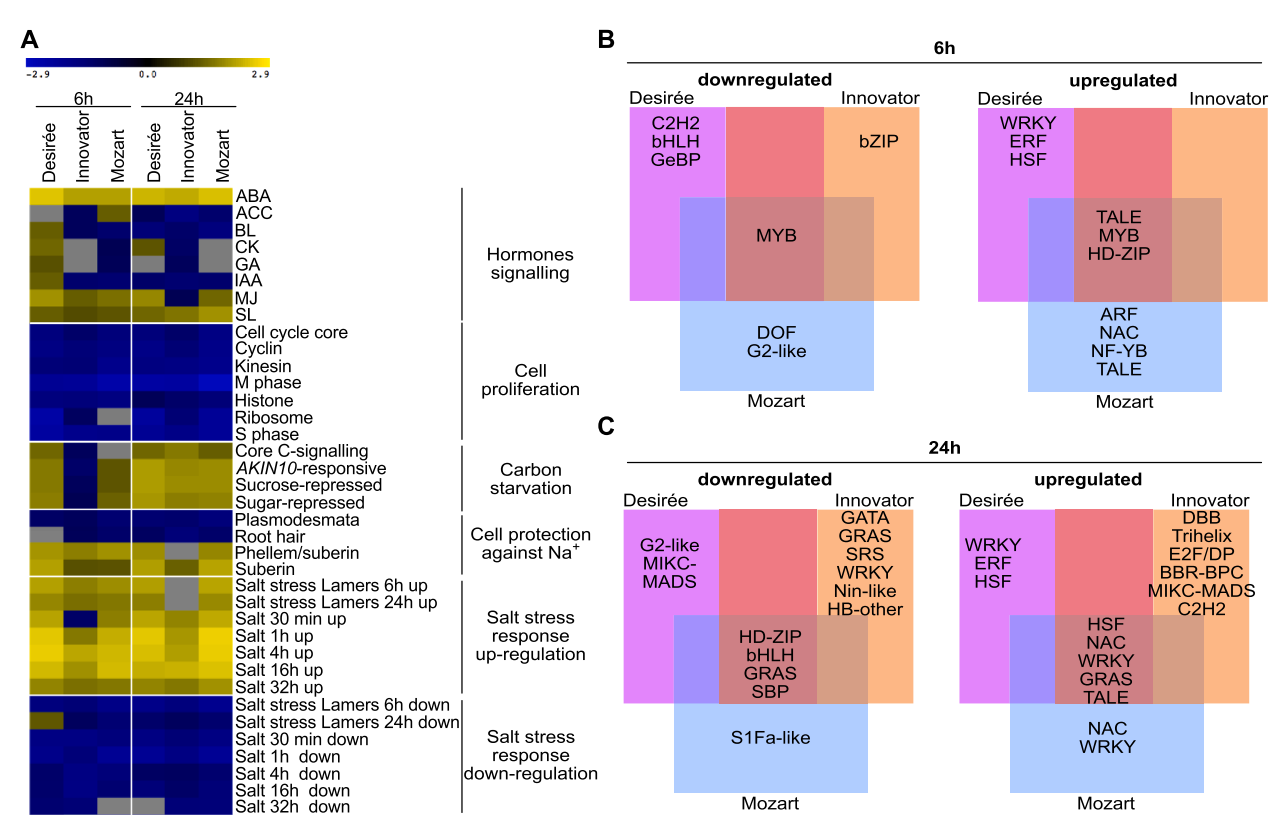


Fig. 4. Genetic pathways involved in root salt stress response in the three cultivars. (A) Heatmap of the Gene Set Enrichment Analysis (GSEA) displaying the normalized enrichment score (NES). GSEA is a statistical approach allowing the identification of over-represented gene sets among the up- and downregulated DEG. Gene sets come from the literature, mostly in Arabidospsis, and available in table S6. Positive NES values (yellow) indicate gene sets which are overrepresented among induced genes (FDR<0.25) and Negative NES values (blue) indicate those which overrepresented among the repressed genes. Null values indicate gene sets not significantly overrepresented and appears in grey (FDR>0.25). (B-C) Venn diagrams showing the transcription factor families overrepresented (P<0.05 in a hypergeometric test) among the up-regulated and down-regulated DEGs in the three cultivars at 6h (B) and 24h (C).

In summary, root suberin and lignin depositions vary between the roots of the cultivars under control conditions. Mozart displays higher levels in the exodermis and Casparian strips even before salt-stress induction. Innovator demonstrated a remarkable ability to acclimate to salt stress by promptly increasing the suberin content from the initial lowest content to a level similar to that of Mozart and limiting its root K^+ loss in response to salt.

3.6. ABA content indicates the degree of salt-stress response and salt acclimation in the three cultivars

ABA is a well-known hormone mediating stress responses in plants (Trivedi et al., 2016). GO Analysis and GSEA indicated an activation of ABA signalling in roots after salt stress (Table 1; Fig. 4A) To confirm its role in salt-stress responses in potato, we measured the ABA content in roots after 6h and 24h. The results confirmed our hypothesis that ABA concentration is increased in salt-treated plants compared to the control (Fig. 5D; Supplementary Table 1). However, the increased concentration of ABA was stronger in Innovator roots at 6h compared to the other cultivars. After 24h of treatment, the level of ABA was equivalent to the control in Desirée and Innovator roots. However, in Mozart the ABA content remained high suggesting that Mozart roots were still in a stress phase after 24h of stress.

After induction of salt stress in the roots, ABA can be transported and/or synthesized in other parts of the plant, for example in leaves (Trivedi et al., 2016). Thus, to study the ABA accumulation pattern in potato cultivars, we also quantified its content in leaves. The results showed that ABA content increased in the three cultivars after 6h (Fig. 5E; Supplementary Table 1). However, the ABA content in the leaves remained significantly higher in the three cultivars compared to

the control after 24h in contrast to the roots. The difference between treated and control plants was actually stronger in Innovator and Mozart suggesting that these two cultivars induced a stronger ABA-related stress response which is consistent with their higher sodium content in the aerial parts (Fig. 2D).

In summary, salt stress induces a transient accumulation of ABA in potato roots after 6h which is substantial in Innovator, suggesting a higher stress in this cultivar likely due to its initial lower suberin deposition and K⁺ leakage. After 24h, ABA accumulation in the aerial part is higher in Innovator and Mozart which may be linked with their increased sodium level.

4. Discussion

This study combined plant phenotyping, physiological, transcriptomic and metabolomics analysis and confocal imaging to explore how three contrasting cultivars respond and acclimate to salt stress. In addition to the classical phenotyping of the leaves and roots, we included the stolons, stolon node roots and tubers, which are usually excluded from such studies in potato. These results showed that cultivars differently respond to salt stress, highlighting different abilities of acclimation and resilience.

4.1. Innovator and Desirée, two distinct responses to salt stress

Determining the most resilient genotype depends on the traits of interest. Potato agronomic utility is based on tuber production. Consequently, tuber yield is a pivotal criterion for identifying resilient potato cultivars. Under salinity stress, Innovator was the most resilient cultivar with minimal tuber yield changes and the highest STI. However, its low

M. Nicolas et al. Plant Stress 15 (2025) 100798

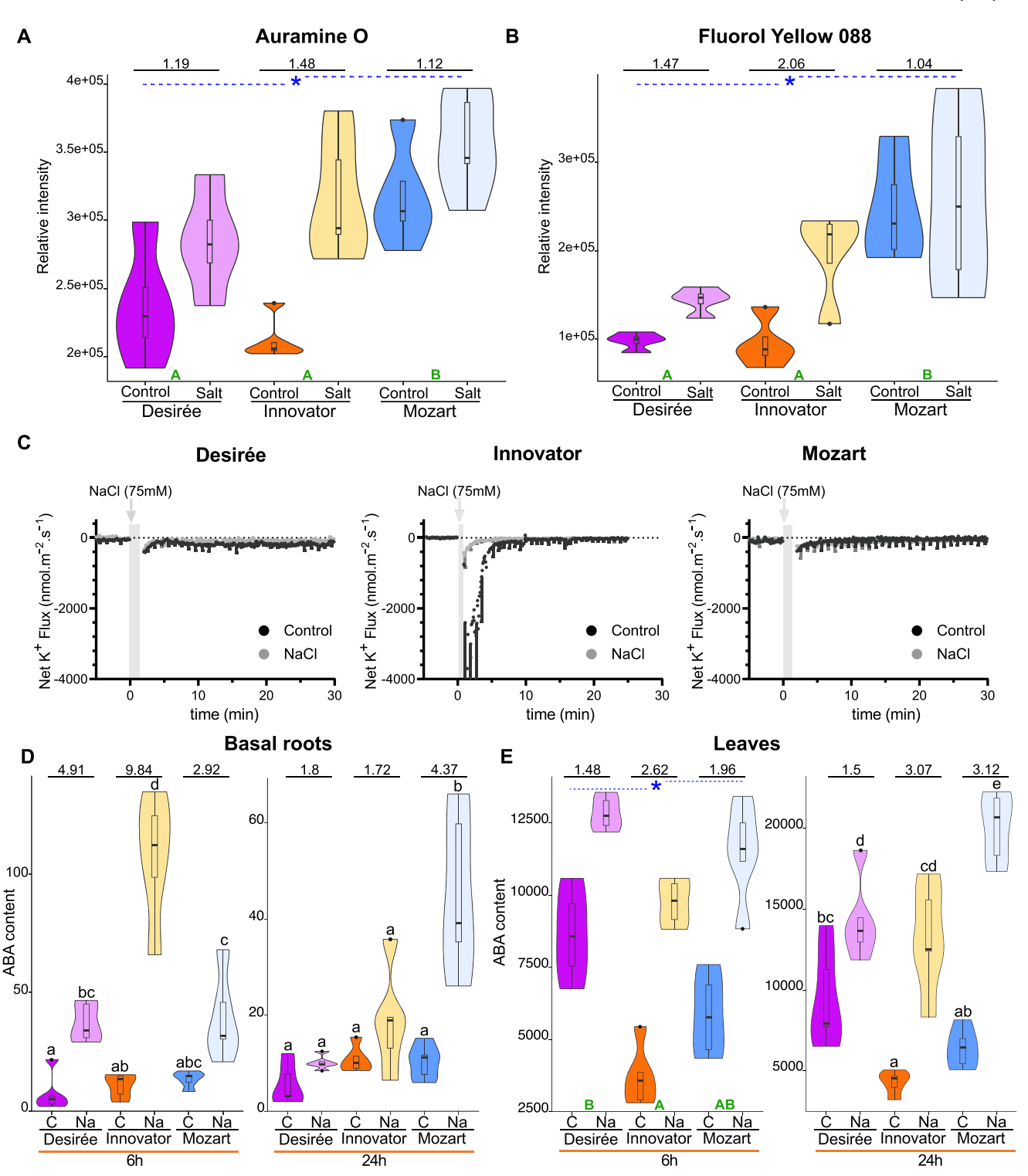


Fig. 5. Plant response to salt stress. (A-B) Quantification of suberin and lignin deposition in the basal root of the three cultivars. 20-day old plants were grown *in vitro* in control or salt stress conditions (125 mM) for one week. Auramine O (lignin and suberin) or Fluorol Yellow 088 (suberin) staining reagents were used (n=5 for Auramine 0 and n=4 for Yellow088, each replicate represents the mean value of 3 roots). (C) K+ flux in basal roots measured in control plants or plants previously stressed (75 mM) for 14 days *in vitro* conditions. Five biological replicates per treatment and genotype were used. Data represent the mean, error bars the standard deviation. For Desiree and Mozart, the null hypothesis that the exponential decay curves used to fit the fluxes after the addition of NaCl are identical for treatment and control roots cannot be rejected. For Innovator, the null hypothesis must be rejected as both the Akaike Information Criterion (AIC) (probability <0.1%, AICc = 21.76) and the extra sum-of-squares F-test (p < 0.0001, F (DFn, DFd) = 28.15 (2, 14)) show that the data should be fitted with two separate curves. (D-E) Violin plots depicting ABA contents in basal roots and leaves of the three cultivars in response to salt stress after 6h and 24h (n = 5 pools of 3 plants). Plants were grown in hydroponic conditions, in either control (C) or in salt stress (Na, 125 mM) environments. ABA values are normalized by fresh weight of the samples. The value above each Control-Salt plot represents the ratio of salt to Control. Lowercase letters indicate differences significant differences among means (Tukey's HSD) when the interaction genotype:treatment was significant (P<0.05). When the interaction is not significant (P>0.05), green capital letters indicate differences between genotypes when significant (P<0.05). Results of the statistical tests are shown in Supplementary Table 1.

original yield compared to Desirée and its low water retention could be disadvantageous under field conditions.

Conversely, Desirée, though showing reduced tuber yield, demonstrated significant resilience with the second-highest STI and the best water retention, which confirms previous findings (Jaarsma et al., 2013). Mozart was the most sensitive genotype and shows the highest Na^+/K^+ ratio in leaves. The higher Na^+ concentration and ABA content in Innovator and Mozart leaves after 24 hours (Fig. 2D) could result from higher water loss due to a higher transpiration stream and hence Na^+ transport to this organ (Asch et al., 2000; Jaarsma et al., 2013).

Suberin and lignin coats, crucial for Na⁺ exclusion in many species (Ranathunge and Schreiber, 2011; Barberon et al., 2016; Karlova et al., 2021; Li et al., 2023), are less deposited in Desirée and Innovator. This potentially leads to a higher root hydraulic conductivity and hence greater absorption of Na⁺ and Cl⁻ ions within the first hours, generating more stress. A SKOR/GORK channel, Soltu.DM.11G001630, is also more expressed in Innovator and could likely be involved in the strong net K⁺ efflux observed in Innovator's control roots (Supplementary Fig. 4). Other identified channels and transporter genes in Innovator are interesting candidates for studying salt-stress acclimation in potato.

In the meanwhile, ABA accumulation may contribute to the compensatory suberin deposition observed at 24h in Innovator and Desirée and hence to the Na $^+$ influx limitation (Barberon et al., 2016; Shukla et al., 2021). In terms of salt-stress resilience, this result indicates that the initial suberin content under control conditions and the associated high root K^+ efflux or loss are less critical than the roots' ability to adequately acclimate to the stress.

4.2. Deciphering the early steps of salt-stress response in potato cultivars

Innovator's ABA and suberin levels, along with K⁺ efflux, suggest a longer root quiescent phase in this cultivar, which could explain its different transcriptomic pattern. After 24h, this delayed salt response might lead to a prompt and substantial transcriptome reprogramming of almost a third of the total gene number, which could explain why sugar starvation and wounding gene sets are not activated after 6h in Innovator. Identification of the molecular mechanisms that enable Innovator to efficiently acclimate to salt stress and maintain a similar yield could be beneficial for improving the yield production of other cultivars, such as Desirée.

Nonetheless, GO and GSEA identified conserved pathways involved in salt-stress response in the three potato cultivars. Besides the expected ABA response, a homogenous activation of strigolactone (SL) pathway was identified. SLs, produced by roots, modulate the root system architecture by inhibiting adventitious and lateral root formations (Rasmussen et al., 2013). Additionally, they can relieve the negative effects of adverse environmental conditions like drought, heat and salt stress in Arabidopsis (Ha et al., 2014; Salvi et al., 2021). MJ, known to increase under abiotic stress conditions and likely to collaborate with ABA, is logically activated across all cultivars after 6h (Salvi et al., 2021). Moreover, MJ can reduce Na⁺/K⁺ ratio in roots and leaves in maize (Rehman et al., 2023) which is consistent with its early activation here. Unexpectedly, the stress-related ethylene pathway (Achard et al., 2006) was inactivated after 24h. However, the loss of function of ethylene receptors ETHYLENE RESPONSE 1 (ETR1) and ETHYLENE INSENSITIVE 4 (EIN4), generate enhanced salt tolerance and ethylene also has a negative effect on suberin deposition and HAK5 expression (Van Zelm et al., 2020; Peng et al., 2014). Consequently, local inactivation of the ethylene pathway could take part in the root recovery phase in potato. The diverse responses of BR, CK, and GA to salt stress among cultivars suggest they have a nuanced role in the stress response. Many gene sets activated in Arabidopsis under salt stress are similarly induced in potato and highlights that salt-stress response is well conserved. Furthermore, induction of phosphate and Fe starvation gene sets upon salt stress aligns with the reduced uptake of essential nutrients due to Na⁺ accumulation in roots and highlights the connection between salt-stress response and nutrient uptake pathways (Parihar et al., 2015). Overall, there is a lower conservation of downregulated gene sets between Arabidopsis and potato which suggests they are more species-specific and likely depend on the transcriptome of the particular cultivar

4.3. An organised regulation of TF activity during salt stress response

Our study reveals a time-specific role of TF families in response to salt stress. In the first hours MYBs undergo significant turnover. MYB is a large family involved in primary and secondary metabolism, cell identity, developmental processes, but also in response to biotic and abiotic stress. Several MYBs were shown to be involved in salt and osmotic stress, suberin deposition, dehydration and phosphate starvation responses and their action is often related to ABA signalling (Li et al., 2023; Shukla et al., 2021; Dubos et al., 2010). Likewise, HD-Zip TF family regulates the expression of downstream stress-related genes through ABA and their role in salt stress has already been pointed out in different species (Ariel et al., 2010; Sharif et al., 2021; Li et al., 2022). In potato, they might play a crucial role in the early stage of the salt stress response before being downregulated after 24h. TALE TFs show consistent upregulation at both time points. A recent model states they might create a permissive chromatin platform permitting the binding of other specific TFs afterwards (Bobola and Sagerström, 2022). We can speculate that salt stress and the implied transcriptome reprogramming hence requires the preliminary action of TALE proteins. The enrichment of HSF and WRKY TF families at 24h suggests their vital role during the later acclimation phase to salt stress.

4.4. Maintenance of a strong sugar sink belowground is a crucial process in potato under stress

Despite its high concentration in stolons, tubers did not accumulate Na^+ . The intense sugar metabolism during tuberization is likely incompatible with Na^+ storage. Furthermore, the increased Cl- and K^+ concentrations in the tubers strongly suggest an active Na^+ exclusion linked to a compensatory K^+ uptake which could involve Na^+ and K^+ transporters like HKT1 and HAK5 (Van Zelm et al., 2020).

Nevertheless, salt can reduce stolon and stolon node root growth and tuber yield as observed in Desirée suggesting this cultivar suffers a lower sugar sink strength belowground in those conditions. This aligns with the growth reduction and the activation of carbon starvation gene sets after salt stress observed in the GO and GSEA analyses. However, basal roots growth was not reduced, possibly due to preliminary growth during the first three weeks prior to salt-stress induction. Immediate salt-stress induction upon tuber planting may accentuate belowground differences.

Potato tubers are located belowground, close to the roots, where salt is absorbed. Therefore, maintaining a sufficient belowground sugar sink is critical for maintaining tuber yield. Despite Desirée showing the highest yield under control conditions, tuber production decreased significantly under salt stress and became similar to Mozart and Innovator. Halophyte species like *Schrenkiella parvula* have more sugar transporter genes to compensate for decreased sugar sink (Zou et al., 2017). Therefore, an increased sugar transport belowground or enhancing starch biosynthesis in tubers may boost yields in cultivars like Desirée.

5. Conclusion

Altogether, we showed that Innovator was the most resilient cultivar, displaying yield stability in salt-stress conditions, due to a high degree of acclimation but displays a more severe water-loss under salt stress. A combination of Desirée's higher yield potential and Innovator's yield stability could be of significant agricultural interest. Absence of Na $^+$ accumulation and K^+ increase in tubers growing under salt stress in the

three cultivars is a remarkable phenomenon that requires further studies and can lead to a better understanding of salt tolerance mechanisms. Our RNA-seq analyses pointed towards different TFs and ion transporters which are interesting candidates for further analysis on the quest of breeding for salt resilience in potato.

Data availability

The data that support the findings of this study are available in the Supporting Information of this article. The sequence data that support the findings of this study are openly available in the BIOSTUDIES database (https://www.ebi.ac.uk/biostudies/) under accession no. E-MTAB-14,181.

CRediT authorship contribution statement

Michael Nicolas: Writing - review & editing, Writing - original draft, Visualization, Validation, Supervision, Methodology, Investigation, Formal analysis, Data curation, Conceptualization. Jort Bouma: Writing - review & editing, Investigation. Jan Henk Venema: Writing review & editing, Supervision, Investigation. Hanneke van der Schoot: Investigation. Francel Verstappen: Methodology, Investigation. Thijs de Zeeuw: Investigation. Sanne E. Langedijk: Writing - review & editing, Investigation. Damian Boer: Writing - review & editing, Investigation. Johan Bucher: Investigation. Marten Staal: Investigation. Ben Krom: Investigation. J. Theo M Elzenga: Writing – review & editing, Methodology, Investigation. Richard G.F. Visser: Writing review & editing, Resources, Funding acquisition, Conceptualization. Christa Testerink: Writing – review & editing, Validation, Supervision, Project administration, Methodology, Funding acquisition, Conceptualization. Rumyana Karlova: Writing - review & editing, Writing original draft, Validation, Supervision, Resources, Project administra-Funding acquisition, Methodology, Formal Conceptualization.

Declaration of competing interest

The authors declare that they have no known competing financial interests or personal relationships that could have appeared to influence the work reported in this paper.

Acknowledgments

This work was supported by the NWO (Grant No. 16893), "Getting to the roots of salt-stress resilience of potato plants". We thank J. Busscher for the lab management at the Plant Physiology laboratory (WUR), S. Geurts and people of Unifarm for their technical assistance in the greenhouse (WUR). We are thankful to Gerard van der Linden (WUR) for useful discussions and Joel Meunier (CNRS IRBI Tours, France) for feedbacks on statistical analyses.

Supplementary materials

Supplementary material associated with this article can be found, in the online version, at doi:10.1016/j.stress.2025.100798.

References

- Achard, P., Cheng, H., Grauwe, L.De, Decat, J., Schoutteten, H., Moritz, T., Van Der Straeten, D., Peng, J., Harberd, N.P, 2006. Integration of plant responses to environmentally activated phytohormonal signals. Science 311, 91–94.
- Ahmed, H.A.A., Şahin, N.K., Akdoğan, G., Yaman, C., Köm, D., Uranbey, S., 2020. Variability in salinity stress tolerance of potato (Solanum tuberosum L.) varieties using *in vitro* screening. Ciência e Agrotecnologia 44, 1–14. Available at: http://www.scielo.br/scielo.php?script=sci_arttext&pid=S1413-70542020000100219&tlng=en
- Alexa, A. and Rahnenfuhrer, J. (2023) topGO: Enrichment Analysis for Gene Ontology. Available at: https://bioconductor.org/packages/topGO.

- Andrews, S., 2010. FastQC: A Quality Control Tool for High Throughput Sequence Data. Available online at: http://www.bioinformatics.babraham.ac.uk/projects/fastqc/and https://github.com/s-andrews/FastQC.
- Ariel, F., Diet, A., Verdenaud, M., Gruber, V., Frugier, F., Chan, R., Crespi, M., 2010. Environmental regulation of lateral root emergence in medicago truncatula requires the HD-Zip I transcription factor HB1. Plant Cell 22, 2171–2183. Available at: https://academic.oup.com/plcell/article/22/7/2171/6095961.
- Asch, F., Dingkuhn, M., Dörffling, K., Miezan, K., 2000. Leaf K/Na ratio predicts salinity induced yield loss in irrigated rice. Euphytica 109–118.
- Baena-González, E., Rolland, F., Thevelein, J.M., Sheen, J., 2007. A central integrator of transcription networks in plant stress and energy signalling. Nature 448, 938–942.
- Barberon, M., Vermeer, J.E.M., Bellis, D.De, et al., 2016. Adaptation of root function by nutrient-induced plasticity of endodermal differentiation. Cell 164, 447–459. https://doi.org/10.1016/j.cell.2015.12.021. Available at:
- Bobola, N., Sagerström, C.G., 2022. TALE transcription factors: cofactors no more. Semin. Cell Dev. Biol. 153, 76–84.
- Brault, M.L., Petit, J.D., Immel, F., et al., 2019. Multiple C2 domains and transmembrane region proteins (MCTPs) tether membranes at plasmodesmata. EMBO Rep. 20, e47182. Available at: https://onlinelibrary.wiley.com/doi/abs/10.15252/embr.201 847182.
- Briggs, C.L., Morris, E.C., 2008. Seed-coat dormancy in Grevillea linearifolia: Little change in permeability to an apoplastic tracer after treatment with smoke and heat. Ann. Bot. 101, 623–632.
- Calvo-Polanco, M., Ribeyre, Z., Dauzat, M., et al., 2021. Physiological roles of Casparian strips and suberin in the transport of water and solutes. New Phytol. 232, 2295–2307
- Cavanaugh, J.E., Neath, A.A., 2019. The Akaike information criterion: Background, derivation, properties, application, interpretation, and refinements. WIREs Comput. Stat. 11, 1–11. Available at: https://wires.onlinelibrary.wiley.com/doi/10.1002/wics.1460.
- Dahal, K., Li, X.Q., Tai, H., Creelman, A., Bizimungu, B., 2019. Improving potato stress tolerance and tuber yield under a climate change scenario – a current overview. Front. Plant Sci. 10.
- Dasgupta, S., Laplante, B., Meisner, C., Wheeler, D., Yan, J., 2009. The impact of sea level rise on developing countries: a comparative analysis. Clim. Change 93, 379–388. Available at: http://link.springer.com/10.1007/s10584-008-9499-5.
- Dinneny, J.R., Long, T.A., Wang, J.Y., et al., 2008. Cell identity mediates the response of Arabidopsis roots to abiotic stress. Science 320, 942–945.
- Doblas, V.G., Geldner, N., Barberon, M., 2017. The endodermis, a tightly controlled barrier for nutrients. Curr. Opin. Plant Biol. 39, 136–143.
- Duan, L., Dietrich, D., Ng, C.H., Yeen Chan, P.M., Bhalerao, R., Bennett, M.J., Dinneny, J. R., 2013. Endodermal ABA signaling promotes lateral root quiescence during salt stress in Arabidopsis seedlings. Plant Cell 25, 324–341.
- Dubos, C., Stracke, R., Grotewold, E., Weisshaar, B., Martin, C., Lepiniec, L., 2010. MYB transcription factors in Arabidopsis. Trends Plant Sci. 15, 573–581.
- Ewels, P., Magnusson, M., Lundin, S., Käller, M., 2016. MultiQC: summarize analysis results for multiple tools and samples in a single report. Bioinformatics 32, 3047–3048.
- Ewing, E.E., Struik, P.C., 1992. Tuber formation in potato: induction, initiation, and growth. Horticultural Reviews. John Wiley & Sons, Inc., Oxford, UK, pp. 89–198. Available at: http://doi.wiley.com/10.1002/9780470650523.ch3.
- FAO, WFP, IFAD, UNICEF and WHO, 2017. The State of Food Security and Nutrition in the World 2017. FAO, Rome. Available at: https://openknowledge.fao.org/items/0f 85cf59-0370-461b-9481-f0f708ed024d.
- Floková, K., Tarkowská, D., Miersch, O., Strnad, M., Wasternack, C., Novák, O., 2014. UHPLC—MS/MS based target profiling of stress-induced phytohormones. Phytochemistry 105, 147–157. Available at: https://linkinghub.elsevier.com/retrie/ve/nii/S003194221400226X.
- Ghosh, S.C., Asanuma, K.I., Kusutani, A., Toyota, M., 2001. Effect of salt stress on some chemical components and yield of potato. Soil Sci. Plant Nutr. 47, 467–475.
- Gifford, M.L., Dean, A., Gutierrez, R.A., Coruzzi, G.M., Birnbaum, K.D., 2008. Cell-specific nitrogen responses mediate developmental plasticity. Proc. Natl. Acad. Sci 105, 803–808. Available at: https://pnas.org/doi/full/10.1073/pnas.0709559105.
- Gonzali, S., Loreti, E., Solfanelli, C., Novi, G., Alpi, A., Perata, P., 2006. Identification of sugar-modulated genes and evidence for *in vivo* sugar sensing in Arabidopsis. J. Plant Res. 119, 115–123.
- Gühl, K., Holmer, R., Xiao, T.T., Shen, D., Wardhani, T.A.K., Geurts, R., Zeijl, A., van and Kohlen, W., 2021. Accumulation, and nodule initiation in medicago truncatula. Genes (Basel) 12, 988.
- Ha, C.Van, Leyva-Gonzalez, M.A., Osakabe, Y., et al., 2014. Positive regulatory role of strigolactone in plant responses to drought and salt stress. Proc. Natl. Acad. Sci. U. S. A. 111, 851–856
- Hartig, F., 2024. DHARMa: residual diagnostics for hierarchical (multi-level /mixed) regression models. CRAN Contrib. Packag. Available at: https://cran.r-project.org/package=DHARMa.
- Hassani, A., Azapagic, A., Shokri, N., 2020. Predicting long-term dynamics of soil salinity and sodicity on a global scale. Proc. Natl. Acad. Sci. U. S. A. 117, 33017–33027.
- Ho, L.C., 1988. Metabolism and compartmentation of imported sugars in sink organs in relation to sink strength. Annu. Rev. Plant Physiol. Plant Mol. Biol. 39, 355–378. Available at: http://www.annualreviews.org/doi/10.1146/annurev.pp.39.060188. 002035
- Hothorn, T., Bretz, F., Westfall, P., 2025. Multcomp: simultaneous inference in general parametric models. CRAN Contrib. Packag. Available at: https://cran.r-project. org/package=multcomp.
- Houtman, C.J., Kitin, P., Houtman, J.C.D., Hammel, K.E., Hunt, C.G., 2016. Acridine orange indicates early oxidation of wood cell walls by fungi. PLoS One 11, 1–19.

- Huang, L., Shi, X., Wang, W., Ryu, K.H., Schiefelbein, J., 2017. Diversification of root hair development genes in vascular plants. Plant Physiol 174, 1697–1712.
- Ivushkin, K., Bartholomeus, H., Bregt, A.K., Pulatov, A., Kempen, B., Sousa, L.de, 2019. Global mapping of soil salinity change. Remote Sens. Environ. 231, 111260. https://doi.org/10.1016/j.rse.2019.111260. Available at:
- Iyer-Pascuzzi, A.S., Jackson, T., Cui, H., Petricka, J.J., Busch, W., Tsukagoshi, H., Benfey, P.N., 2011. Cell identity regulators link development and stress responses in the arabidopsis root. Dev. Cell 21, 770–782. https://doi.org/10.1016/j. devcel.2011.09.009. Available at:
- Jaarsma, R., Boer, A.H.de, 2018. Salinity tolerance of two potato cultivars (Solanum tuberosum) correlates with differences in vacuolar transport activity. Front. Plant Sci. 9, 1–12
- Jaarsma, R., Vries, R.S.M.de, Boer, A.H.de, 2013. Effect of salt stress on growth, Na+ accumulation and proline metabolism in potato (solanum tuberosum) cultivars. PLoS One 8
- Karlova, R., Boer, D., Hayes, S., Testerink, C., 2021. Root plasticity under abiotic stress. Plant Physiol 1–14. Available at: https://academic.oup.com/plphys/advance-article/doi/10.1093/plphys/kiab392/6359830.
- Kinoshita, N., Wang, H., Kasahara, H., Liu, J., MacPherson, C., Machida, Y., Kamiya, Y., Hannah, M.A., Chuaa, N.H., 2012. IAA-Ala Resistant3, an evolutionarily conserved target of miR167, mediates Arabidopsis root architecture changes during high osmotic stress. Plant Cell 24, 3590–3602.
- Kováčik, J., Babula, P., Klejdus, B., Hedbavny, J., Jarošová, M., 2014. Unexpected behavior of some nitric oxide modulators under cadmium excess in plant tissue. PLoS One 9, 1–10.
- Kratzke, M.G., Palta, J.P., 1985. Evidence for the existence of functional roots on potato tubers and stolons: Significance in water transport to the tuber. Am. Potato J. 62, 227–236
- Krueger, F., James, F., Ewels, P., Afyounian, E., Weinstein, M., Schuster-Boeckler, B. and Hulselmans, G. (2023) TrimGalore. Available at: https://github.com/FelixKrueger /TrimGalore/tree/0.6.10.
- Kurihara, D., Mizuta, Y., Sato, Y., Higashiyama, T., 2015. ClearSee: a rapid optical clearing reagent for whole-plant fluorescence imaging. Development 4168–4179. Available at: http://dev.biologists.org/cgi/doi/10.1242/dev.127613.
- Lamers, J., Van Der Meer, T., Testerink, C., 2020. How plants sense and respond to stressful environments. Plant Physiol. 182, 1624–1635.
- Lamers, J., Zhang, Y., Zelm, E. Van, et al. (2023) Abscisic acid signaling gates saltspecific responses of plant roots. bioRxiv, 1–28.
- Lan, P., Li, W., Schmidt, W., 2012. Complementary proteome and transcriptome profiling in phosphate-deficient arabidopsis roots reveals multiple levels of gene regulation. Mol. Cell. Proteomics 11, 1156–1166. https://doi.org/10.1074/mcp.M112.020461. Available at:
- Leal, A.R., Barros, P.M., Parizot, B., Sapeta, H., Vangheluwe, N., Andersen, T.G., Beeckman, T., Oliveira, M.M., 2022. Translational profile of developing phellem cells in Arabidopsis thaliana roots. Plant J. 110, 899–915. Available at: https://onlinelibrary.wiley.com/doi/10.1111/tpi.15691.
- Lenth, R.V., 2017. Emmeans: estimated marginal means, aka least-squares means. CRAN Contrib. Packag. Available at: https://cran.r-project.org/package=emmeans.
- Lex, A., Gehlenborg, N., Strobelt, H., Vuillemot, R., Pfister, H., 2014. UpSet: visualization of intersecting sets. IEEE Trans. Vis. Comput. Graph. 20, 1983–1992. https://doi. org/10.1109/TVCG.2014.2346248.
- Li, H., Duijts, K., Pasini, C., et al., 2023. Effective root responses to salinity stress include maintained cell expansion and carbon allocation. New Phytol. 238, 1942–1956. Available at: https://nph.onlinelibrary.wiley.com/doi/10.1111/nph.18873.
- Li, W., Lan, P., 2015. Genome-wide analysis of overlapping genes regulated by iron deficiency and phosphate starvation reveals new interactions in Arabidopsis roots. BMC Res. Notes 8, 1–16.
- Li, K., Reeve, D.W., 2004. Fluorescent labeling of lignin in the wood pulp fiber wall. J. Wood Chem. Technol. 24, 169–181. https://doi.org/10.1081/WCT-200026572.
- Li, Y., Yang, Z., Zhang, Y., Guo, J., Liu, L., Wang, C., Wang, B., Han, G., 2022. The roles of HD-ZIP proteins in plant abiotic stress tolerance. Front. Plant Sci. 13, 1–19.
- Love, M.I., Huber, W., Anders, S., 2014. Moderated estimation of fold change and dispersion for RNA-seq data with DESeq2. Genome Biol. 15, 550. Available at: http ://genomebiology.biomedcentral.com/articles/10.1186/s13059-014-0550-8.
- Motulsky, H., Christopoulos, A., 2004. Fitting Models to Biological Data Using Linear and Nonlinear Regression. Oxford University Press, New York, NY. https://doi.org/10.1093/oso/9780195171792.001.0001. Available at:
- Motulsky, H.J., Brown, R.E., 2006. Detecting outliers when fitting data with nonlinear regression - a new method based on robust nonlinear regression and the false discovery rate. BMC Bioinformatics 7, 1–20.
- Nawaz, K., Hussain, K., Majeed, A., Khan, F., Afghan, S., Ali, K., 2010. Fatality of salt stress to plants: morphological, physiological and biochemical aspects. African J. Biotechnol. 9, 5475–5480.
- Nguyen, V.L., Ribot, S.A., Dolstra, O., Niks, R.E., Visser, R.G.F., van der Linden, C.G., 2013. Identification of quantitative trait loci for ion homeostasis and salt tolerance in barley (Hordeum vulgare L.). Mol. Breed. 31, 137–152.
- Nicolas, M., Torres-Pérez, R., Wahl, V., et al., 2022. Spatial control of potato tuberization by the TCP transcription factor BRANCHED1b. Nat. Plants 8, 281–294. Available at: https://www.nature.com/articles/s41477-022-01112-2.
- Osuna, D., Usadel, B., Morcuende, R., et al., 2007. Temporal responses of transcripts, enzyme activities and metabolites after adding sucrose to carbon-deprived Arabidopsis seedlings. Plant J. 49, 463–491.

- Parihar, P., Singh, S., Singh, R., Singh, V.P., Prasad, S.M., 2015. Effect of salinity stress on plants and its tolerance strategies: a review. Environ. Sci. Pollut. Res. 22, 4056–4075.
- Patro, R., Duggal, G., Love, M.I., Irizarry, R.A., Kingsford, C., 2017. Salmon provides fast and bias-aware quantification of transcript expression. Nat. Methods 14, 417–419.
- Peng, J., Li, Z., Wen, X., Li, W., Shi, H., Yang, L., Zhu, H., Guo, H., 2014. Salt-induced stabilization of EIN3/EIL1 confers salinity tolerance by deterring ROS accumulation in arabidopsis. PLoS Genet. 10.
- Pham, G.M., Hamilton, J.P., Wood, J.C., Burke, J.T., Zhao, H., Vaillancourt, B., Ou, S., Jiang, J., Buell, C.R., 2020. Construction of a chromosome-scale long-read reference genome assembly for potato. Gigascience 9, 1–11. Available at: https://academic. oup.com/gigascience/article/doi/10.1093/gigascience/giaa100/5910251.
- Ranathunge, K., Schreiber, L., 2011. Water and solute permeabilities of Arabidopsis roots in relation to the amount and composition of aliphatic suberin. J. Exp. Bot. 62, 1061–1074
- Rasmussen, A., Depuydt, S., Goormachtig, S., Geelen, D., 2013. Strigolactones fine-tune the root system. Planta 238, 615–626.
- Rehman, M., Saeed, M.S., Fan, X., et al., 2023. The multifaceted role of jasmonic acid in plant stress mitigation: an overview. Plants 12.
- Rymen, B., Kawamura, A., Lambolez, A., et al., 2019. Histone acetylation orchestrates wound-induced transcriptional activation and cellular reprogramming in Arabidopsis. Commun. Biol. 2, 1–15. https://doi.org/10.1038/s42003-019-0646-5. Available at:
- Salvi, P., Manna, M., Kaur, H., Thakur, T., Gandass, N., Bhatt, D., Muthamilarasan, M., 2021. Phytohormone signaling and crosstalk in regulating drought stress response in plants. Plant Cell Rep. 40, 1305–1329. https://doi.org/10.1007/s00299-021-02683-8. Available at:
- Schiessl, K., Lilley, J.L.S., Lee, T., et al., 2019. Nodule inception recruits the lateral root developmental program for symbiotic nodule organogenesis in Medicago truncatula. Curr. Biol. 29, 3657–3668. https://doi.org/10.1016/j.cub.2019.09.005 e5Available
- Schindelin, J., Arganda-Carreras, I., Frise, E., et al., 2012. Fiji: an open-source platform for biological-image analysis. Nat. Methods 9, 676–682.
- Shahid, S.A., Zaman, M., Heng, L., 2018. Soil salinity: historical perspectives and a world overview of the problem. Guideline for Salinity Assessment, Mitigation and Adaptation Using Nuclear and Related Techniques. Springer International Publishing, Cham, pp. 43–53. Available at: http://link.springer.com/10.1007/978-3-319-96190-3
- Sharif, R., Raza, A., Chen, P., Li, Y., El-ballat, E.M., Rauf, A., Hano, C., El-esawi, M.A., 2021. Hd-zip gene family: potential roles in improving plant growth and regulating stress-responsive mechanisms in plants. Genes (Basel). 12.
- Shukla, V., Han, J.-P., Cléard, F., et al., 2021. Suberin plasticity to developmental and exogenous cues is regulated by a set of MYB transcription factors. Proc. Natl. Acad. Sci. 118, e2101730118. https://doi.org/10.1101/2021.01.27.428267. Available at:
- Smith, A.M., Stitt, M., 2007. Coordination of carbon supply and plant growth. Plan. Cell Environ. 30, 1126–1149.
- Sonnewald, U., Fernie, A.R., 2018. Next-generation strategies for understanding and influencing source–sink relations in crop plants. Curr. Opin. Plant Biol. 43, 63–70. https://doi.org/10.1016/j.pbi.2018.01.004. Available at:
- Staal, M., Cnodder, T.de, Simon, D., Vandenbussche, F., van der Straeten, D., Verbelen, J. P., Elzenga, T., Vissenberg, K., 2011. Apoplastic alkalinization is instrumental for the inhibition of cell elongation in the Arabidopsis root by the ethylene precursor 1-aminocyclopropane-1-carboxylic acid. Plant Physiol. 155, 2049–2055.
- Subramanian, A., Tamayo, P., Mootha, V.K., et al., 2005. Gene set enrichment analysis: A knowledge-based approach for interpreting genome-wide expression profiles. Proc. Natl. Acad. Sci. U. S. A. 102. 15545–15550.
- Sulpice, R., Pyl, E.-T., Ishihara, H., et al., 2009. Starch as a major integrator in the regulation of plant growth. Proc. Natl. Acad. Sci 106, 10348–10353. Available at: http://www.pnas.org/cgi/doi/10.1073/pnas.0903478106.
- Tarancón, C., González-Grandío, E., Oliveros, J.C., Nicolas, M., Cubas, P., 2017.
 A conserved carbon starvation response underlies bud dormancy in woody and herbaceous species. Front. Plant Sci. 8, 1–21. Available at: http://journal.frontiersin.org/article/10.3389/fpls.2017.00788/full [Accessed June 20, 2017].
- Trivedi, D.K., Gill, S.S., Tuteja, N., 2016. Abscisic acid (ABA): biosynthesis, regulation, and role in abiotic stress tolerance. Abiotic Stress Response in Plants. Wiley, pp. 315–326. Available at: https://onlinelibrary.wiley.com/doi/10.1002/9783527694570.ch15.
- Ursache, R., Andersen, T.G., Marhavý, P., Geldner, N., 2018. A protocol for combining fluorescent proteins with histological stains for diverse cell wall components. Plant J. 93, 399–412
- Van Zelm, E., Zhang, Y., Testerink, C., 2020. Salt tolerance mechanisms of plants. Annu. Rev. Plant Biol. 71, 403–433.
- Wickham, H., Chang, W., Henry, L., et al., 2024. ggplot2: create elegant data visualisations using the grammar of graphics. CRAN Contrib. Packag. Available at: https://cran.r-project.org/package=ggplot2.
- Zou, C., Chen, A., Xiao, L., et al., 2017. A high-quality genome assembly of quinoa provides insights into the molecular basis of salt bladder-based salinity tolerance and the exceptional nutritional value. Cell Res 27, 1327–1340. https://doi.org/10.1038/ cr.2017.124. Available at:
- Zou, Y., Zhang, Y., Testerink, C., 2022. Root dynamic growth strategies in response to salinity. Plant. Cell Environ. 45, 695–704. Available at: https://onlinelibrary.wiley. com/doi/10.1111/pce.14205.